DEMOCRATIC AND PEOPLE'S REPUBLIC OF ALGERIA
MINISTRY OF HIGHER EDUCATION AND SCIENTIFIC RESEARCH

Kasdi Merbah University –Ouargla-
Faculty of Mathematics and Material Science
Chemistry Department

Graduation note to obtain a certificate Academic Master

In Chemistry Specialty: applied chemistry

Prepared by: **Ben Aissa yousef**

Under the title:

Modeling and study of application in corrosion inhibition of some synthetic aromatic amines

This thesis was successfully defended on June 20th, 2021 and approved by:

Committee members:

Ali	**DOUADI**	**Pr.**	**UKMO**	**President**
Messouda	**ALLAOUI**	**MCA**	**UKMO**	**Examiner**
Oumelkheir	**RAHIM**	**MCA**	**UKMO**	**Supervisor**

2020/2021

Acknowledgement

The author is thankful to Prof. Dr. Oumelkheir Rahim, Department of Chemistry, Kasdi Merbah University–Ouargla, for the facilities provided, and to all promo of 2020/2021.

Pr. Ali DOUADI, Department of Chemistry, Kasdi Merbah University–Ouargla, for the Accept discussion of the work and correct it to be better, 2020/2021.

Dr. Messouda ALLAOUI, Department of Chemistry, Kasdi Merbah University–Ouargla, for the Accept discussion of the work and correct it to be better, 2020/2021.

List of tables

List of figures

List of abbreviations

Abbreviation	Significance	Page
RMS	Root Mean Square	54
Amber99	Assisted Model Building and Energy Refinement	54
B3LYP	Becke-3 Parameter-Lee-Yang-Parr	54
DFT	Density Functional Theory	54
LanL2DZ	Los Alamos National Laboratory 2 Double Zeta	54
MM+	Molecular mechanics	54
QSAR	Quantitative structure - activity relationships	54
ZINDO1	Dr. Michael Zerner's INDO versions (Intermediate Neglect of Differential Overlap)	54
H.a.u	Hartree atomic unit	56
Log P	Octanol-Water Partition Coefficient	56
XRD	X-Ray Diffraction	59
XRF	X-Ray Fluorescence	59
PIXE	Proton-Induced X-ray Emission	59

Contents

Abstract:

Three ferrocenyl amines derivatives, Fc-1, Fc-2 and Fc-3, have been studded their corrosion inhibition property against corrosion of XC70 steel in 1 M HCl solution at 298 K using electrochemical impedance spectroscopy (EIS) measurements and adsorption isotherms which compared with previous studies, also Quantum chemical calculation have been used to determine Geometry Optimization and estimate stabilization energy, Molecular Mechanic (MM+) and Ab-Initio methods have been carried out for the title compounds, by using HyperChem 8.08 program. Density Functional Theory (DFT) was used with B3LYP hybrid function which coupled with LanL2DZ and 6-31G (d,p) basis set by using Gaussian 09W program.

Keywords: Ferrocene, Ferrocenyl amines derivatives, Corrosion inhibition, EIS, adsorption isotherms, MM+, Ab-Initio, DFT.

ملخص:

ثلاثة مشتقات لفيروسينيل الأمين Fc-1, Fc-2 and Fc-3, تم دراسة خصائص تثبيط التآكل ضد تآكل الفولاذ XC70 في محلول 1 مولارى من حمض الهيدروكلوريك عند 298 كلفن باستخدام قياسات التحليل الطيفي للممانعة الكهروكيميائية (EIS)، وكذلك تم إجراء دراسة الامتزاز بدراسة نماذج الإزوثارم الإمتزاز المتساوي الحرارة، ومقارنتها بالدراسات السابقة، وكذلك استعملت الحسابات الكمية الكيميائية لتحديد الهيئة الاكثر استقرارا و استنتاج طاقة الاستقرار، تم دراسة المركبات باستعمال طريقة Molecular Mechanic (MM+) و Ab-Initio عن طريق برنامج HyperChem 8.08، و استعملت نظرية الدالة الوظيفية للكثافة (DFT) والمتمثلة في الدالة الهجينة B3LYP مع مجموعتي الاساس LanL2DZ و 6-31G (d,p) وذلك باستعمال برنامج Gaussian 09W.

الكلمات المفتاحية: الفيروسان، المشتقات الفيروسينية الأمينية، تثبيط التآكل، EIS، إيزوثارم الإمتزاز، MM+، Ab-Initio، DFT .

摘要：

三种二茂铁胺衍生物， Fc-1、Fc-2 和 Fc- 3。已经使用电化学阻抗谱 (EIS) 测量和吸附等线 线研究了 XC70 钢在 298 K 的 1 M HCL 溶液中对 XC70 钢的腐蚀抑制性能，并与以前的研究相比，还 使用量子化学计算来确定几何优化并使用 HyperChem 8.08 程序对标题化合物进行了分子力学 (MM+) 和 Ab-Initio 方法并估计了稳定能。 密度泛函理论 (DFT) 与 B3LYP 混合函数一起使用，该混合函数与 LanL2DZ 和使用 Gaussian 09W 程序的 6-31G(d,p) 基组耦合。

关键词：二茂铁，二茂铁胺衍生物，腐蚀抑制，EIS，吸附等温线，MM+，Ab-Initio，DFT。

General introduction:

One of the most important things that occurred in the nineties of the last century, where it was and still is the defining mark of our times, which the old continent in particular and the world as a whole witnessed, and which is the source of all the developments that the world is witnessing at the present time, namely the industrial revolution, which took place Fold the paper of the Age of Darkness and open a book of a new era, which is the Renaissance.

The industrial revolution that the world witnessed in the last century brought about great progress in various fields, especially the industrial ones, leading to a huge leap, and with modern technology, man was able to take his first steps on the moon, and then travel to space and explore his worlds and dive in The structure of matter, wandering with electrons, revealing minute particles, and discovering previously unexplored minerals, which by mixing them together obtain metallic alloys, with unique properties that enable the construction of unparalleled factories and buildings.

Steel, the best metal alloy that was manufactured, and it is a metal consisting of different transition metals, most of them, and in different proportions, which give the alloy its unique characteristics of hardness, lightness and durability, which are used widely, especially in the field of industry, where it is used, For example, in the field of energy to transport gas and oil, and there are also those who use them as containers. One of the most prominent problems and phenomena that metal alloys suffer from is the phenomenon of corrosion, which is the problem of the times that refuses to be solved, so that it is fought by various means and methods, it is considered one of the longest types of wars, which are formed due to cleaning them with corrosive substances such as: acids and bases Not to mention the chemicals they contain and the environment conditions to which they are exposed, and among the most important stainless alloys that have been manufactured, including:

High Strength Low Alloy (HSLA) steel, i,e. , API X120 [3], XC 70 [2], aluminum alloy AA2219-T7 [4], and difference mild steel specimens [5-7].

The phenomenon of corrosion is a natural and automatic phenomenon that occurs for all minerals, except for some of them, under certain conditions, during which the mineral seeks to stabilize. There are many different types of corrosion, including galvanic, chemical and local corrosion, and one of the most dangerous types is pitting corrosion, the danger of which is the impossibility of anticipating it and the difficulty of identifying and analyzing it. To reduce this phenomenon, several methods and tactics have been used for this, and the most prominent of which is the use of inhibitors, especially organic ones, which have been very popular in the world, some of which have been used for a long time and some of them are recent in use. Among the unique organo-metallic compounds that have

received great attention in recent years and which are under study, we find Ferrocene and its derivatives, whose structure contains an iron (Fe) atom. Among these studies we find:

M.S. Morad, A.A.O. Sarhan. [8] 2008, S.R. Gupta et al. [9] 2014, S. Fatima et al. [6] 2019, Uzma N et al. [4] 2020,

First chapter: In this chapter, ferrocene compound and its derivatives were briefed, starting from the date of its discovery and passing through the discussion station, which was about the type of iron atom hybridization specified for the spatial structure of the compound, and familiarized with its chemical and physical properties, and ending some areas in which its derivatives are used.

The second and third chapters revolve around a comparative theoretical study of ferrocene derivative that were synthesizes by Rahim, O., et al. [2], they are studied their electrochemical properties using Electrochemical Impedance Spectroscopy (EIS) as inhibitors for mild steel corrosion in 1 M HCl, so as, Adsorption Isotherm, and compared with some previous studies were also discussed.

The fourth chapter is consist of the geometrical optimization of the titled inhibitors that were calculated using quantum chemical software package, and multifarious parameters that indicated by two deferent basis set and compared between them to find which is better one to use for these hybrid organo-metallic systems (HOMS) compounds.

The study contains three indexes:

The first one: demonstrate various parameters that revealed by Electrochemical impedance spectroscopy.

The second one: demonstrate the plots of three Adsorption isotherms that used and their fissures using electrochemical impedance spectroscopy parameters. The third one: demonstrate various parameters that revealed by two deferent basis set and the geometrical optimization of the titled inhibitors.

First chapter:

Ferrocene and its derivatives

I.1 Introduction:

The rapid growth of organo-metallic chemistry is often attributed to the discovery of ferrocene and its many analogues (metallocenes).

Around 1950, when S. Miller, J. Tebboth, and J. Tremaine, researchers at British Oxygen, were attempting to synthesize amines from hydrocarbons and nitrogen in a modification of the Haber process. When they tried to react cyclopentadiene with nitrogen at 300 °C, at atmospheric pressure, they were disappointed to see the hydrocarbon react with some source of iron, yielding ferrocene [1, 10].

In 1951, Peter L. Pauson and Thomas J. Kealy attempted to prepare fulvalene ($(C_5H_4)_2$) by oxidative dimerization of cyclopentadiene (C_5H_6). To that end, they reacted the Grignard compound Cyclopentadienyl magnesium bromide in diethyl ether with ferric chloride as an oxidizer [1]. However, instead of the expected fulvalene Fig.1, a, they obtained a light orange powder of "remarkable stability", with the formula $C_{10}H_{10}Fe$ [11, 12]. Pauson and Kealy conjectured that the compound had two cyclopentadienyl groups, each with a single covalent bond from the saturated carbon atom to the iron atom [1], shown in Fig.1, b.

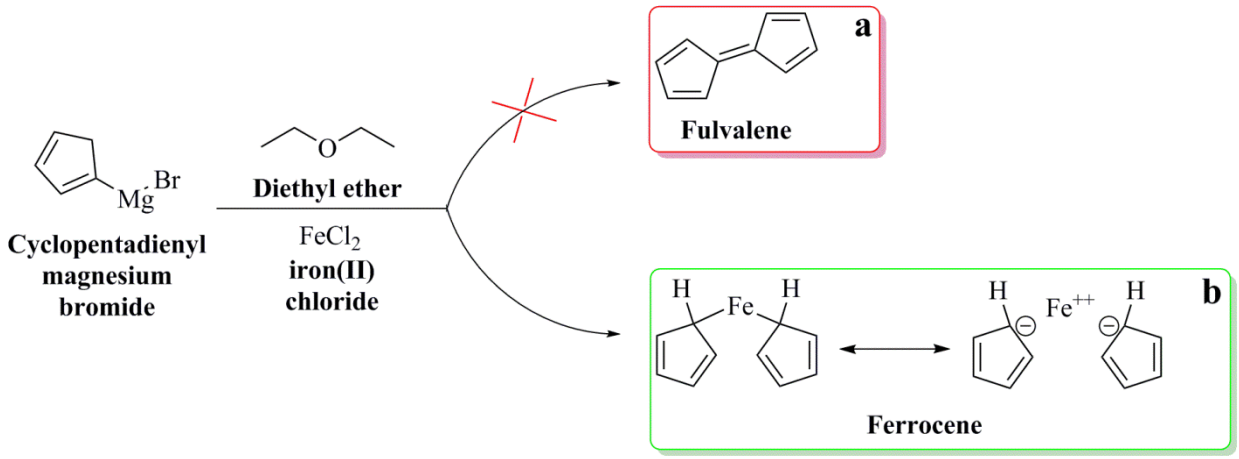

Figure.1. a) Fulvalene the molecule that Pauson and Kealy expected to prepare in 1951, b) Pauson and Kealy's original (incorrect) notion of ferrocene's molecular structure [1].

The English chemist Wilkinson Geoffrey and physicist Ernest Fisher played an important role in correcting the ferrocene's formula that suggested by Pauson and Kealy. They found that all ten carbon atoms attach to iron atom (Fe) by δ covenant bonds. The molecule consists of two cyclopentadienyl rings bound on opposite sides of a central iron atom, Wilkinson and Woodward proved his Sandwich structure, Fig.2, and called him ferrocene with 'ene' ending, which refers to its aromatization in the same way as Benzene [13, 14].

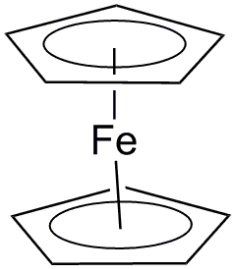

Figure.2. Sandwich structure of ferrocene.

From room temperature down to 164K, X-ray crystallography yields the monoclinic space group; the cyclopentadienide rings are a staggered conformation, resulting in a centrosymmetric molecule, with symmetry group D_{5d} [15], Fig.3, a. However, below 110 K, ferrocene crystallizes in an orthorhombic crystal lattice in which the Cp rings are ordered and eclipsed, so that the molecule has symmetry group D_{5h} [16], Fig.3, b, the Cp rings rotate with a low barrier (~4kJ/mol) about the Cp (centroid) – Fe – Cp (centroid) axis [17].

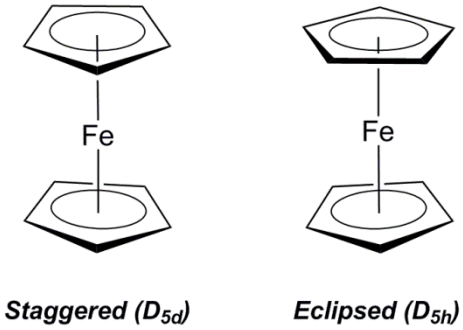

Figure.3. Shows two confirmation of ferrocene
Eclipsed (D_{5d}) and Staggered (D_{5h}).

I.2 Chemical and Physical properties:

Ferrocene's molecular belong to metallocenes, and it is a sandwich-shaped compound with the formula Fe $(C_5H_5)_2$, consisting to cyclopentadienyl rings, linked from opposite sides around the central iron atom [10, 18].

It is a crystalline compound, orange in color, smells like camphor, with a molar mass of 186.04 g/mol, boils at a temperature of 249 °C, its melting point is between 174-173 °C, it is considered a stable compound at high temperatures where it decomposes starting from 400 °C, it is soluble in water 0.1 mg/ml at 21 °C and in DMSO 100 mg/ml at 19.5 °C, and it is soluble in organic solvents such as ether and benzene as well as it is soluble in expanded nitric acid and concentrated sulfuric acid but not soluble in concentrated hydrochloric acid, ferrocene was found to react 3×10^6 times faster than

benzene, and this was confirmed by the electrophilic substitution reaction such as its reaction with aluminum chlorine in the acylation reaction of Friedel-Crafts [13].

I.3 Spectral properties:

I.3.A Hydrogen nuclear magnetic resonance (^{1}H NMR):

Ferrocene gives a single pulse at 4.15ppm, which is representative to the dicyclopentadienyl rings in the proton NMR spectrum [19, 20].

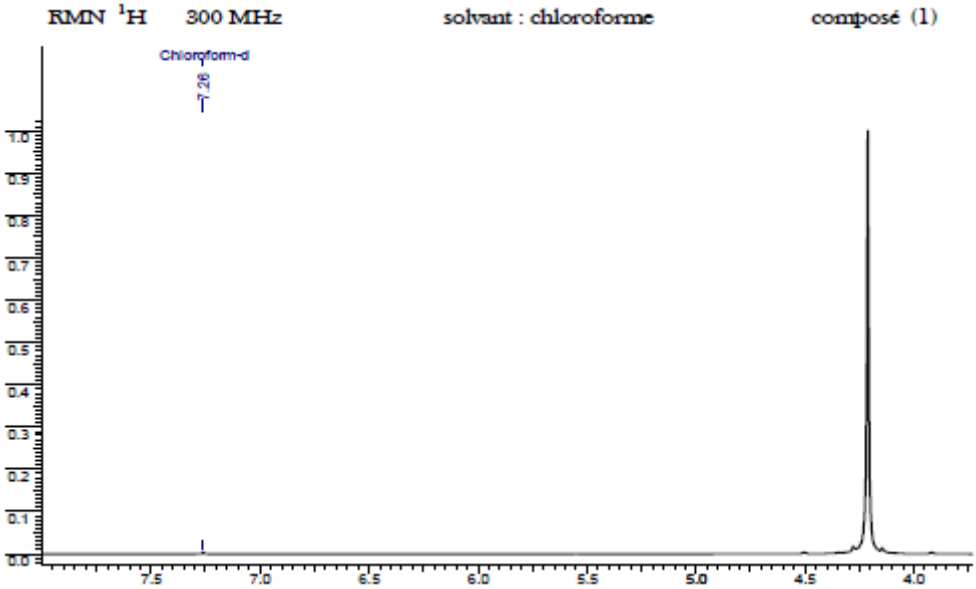

Figure.4. Hydrogen nuclear magnetic resonance (^{1}H NMR) of ferrocene.

I.3.B Carbon nuclear magnetic resonance (^{13}C NMR):

The ferrocene nuclear magnetic resonance (NMR) spectrum contains a single pulse corresponding to the ten carbonates in it [19].

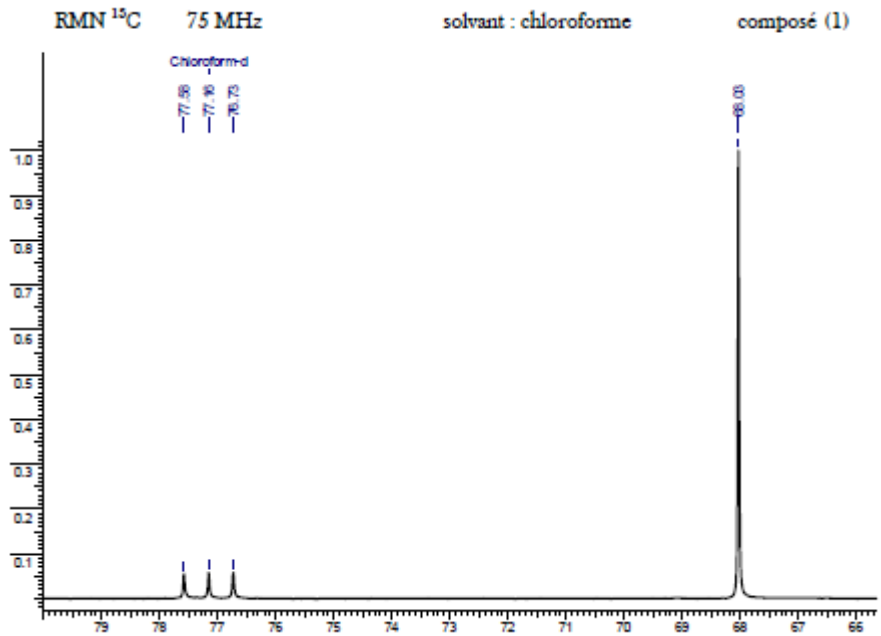

Figure.5. Hydrogen nuclear magnetic resonance (^{13}C NMR) of ferrocene.

I.3.C Infra-red spectroscopy (IR):

For mono-substitution ferrocene, an absorption band of 3075 cm^{-1} appears equivalent to the expansion of the aromatic C–H bond, in addition to the presence of four apparent bands: two of which are 811 cm^{-1} and 1002 cm^{-1} equivalent to the vibration of bending C–H and one 1108 cm^{-1} equivalent to the asymmetric vibration of a ring pentadienyl, and the 1411 cm^{-1} band is equivalent to the asymmetric displacement vibration of the non-substituted pentadienyl ring [17].

I.4 Difference types of metallocenes [21]:

I.4.A Cp_2M Type of metallocenes

Include all neuters metallocenes ($M^{II} = Fe, Ru\ and\ Os$) and mono-cationic ($M^{III} = Co\ and\ Rh$) metallocenes are the complexes d^6 to 18 electrons diamagnetic, Fig.6.

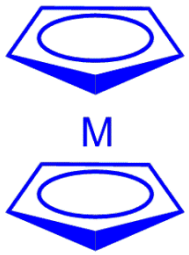

Figure.6. Cp_2M Type of metallocenes.

I.4.B The folded sandwich compounds

In these "curved" metallocenes the two cyclopentadienyl rings are not parallel. There are three species of plaice sandwich compounds which have one, two or three sedimentary ligands, as shown in Fig.7.

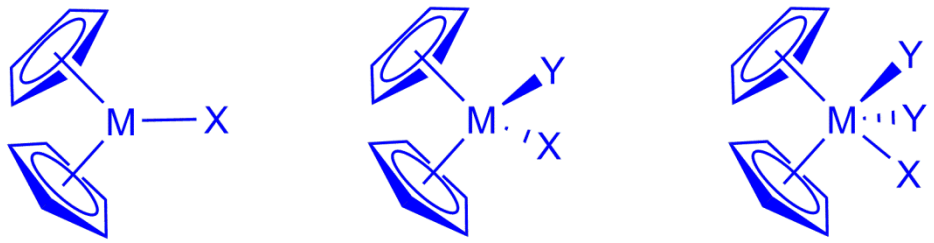

Figure.7. Three species of folded sandwich-type compounds.

Some examples about of folded sandwich-type compounds:

Cp_2FeH^+	Cp_2MoH_2	Cp_2TaH_3
$Cp_2Mo(CO)$	$Cp_2Zr(Cl)H$	$Cp_2Nb(C_2H_4)(Et)$
Cp_2ReH	$Cp_2ReH_2^+$	$Cp_2WH_3^+$

I.4.C Semi-sandwich metallocenes:

These compounds adopt a structure comprising a cyclopentadienyl ring and one to four other ligands. When these ligands are good π acids (such as CO at NO), these complexes are very stable, Fig.8.

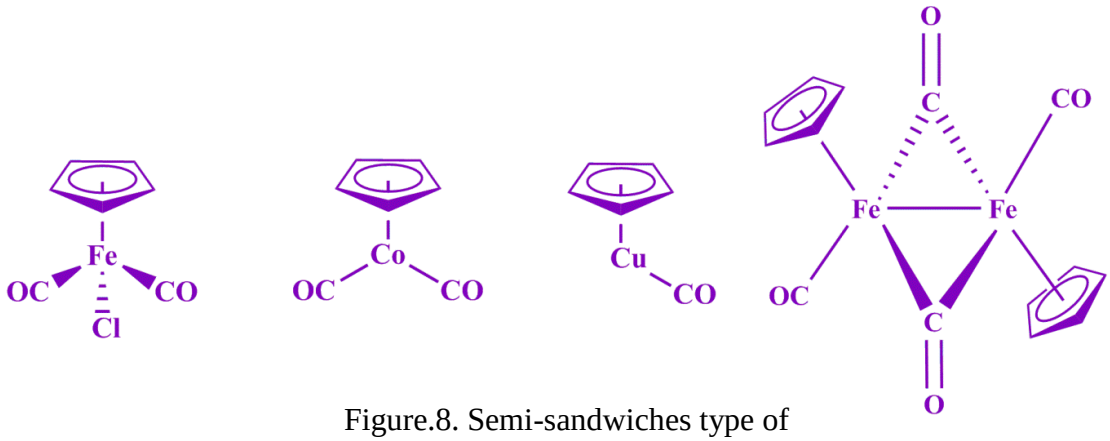

Figure.8. Semi-sandwiches type of metallocenes.

I.4.D Other metallocenes:

In addition to these three categories of metallocenes, there are different types of compounds complexes with the cyclopentadienyl ring, Fig.9. or an heterocyclic analogue, Fig.10.

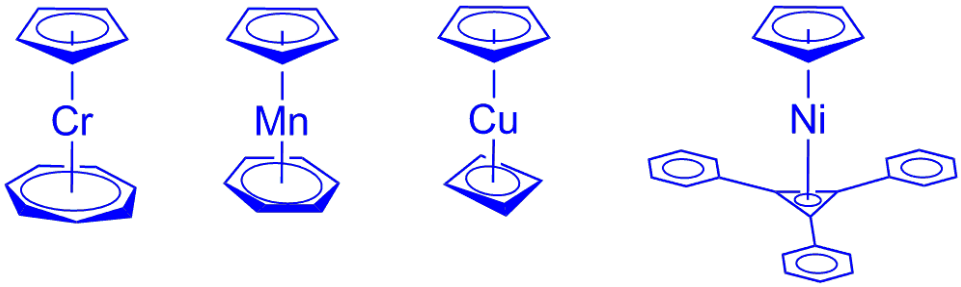

Figure.9. Types of compounds with different in cyclopentadienyl rings.

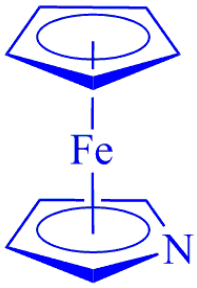

Figure.10. Types of compounds with different atom within the ring of cyclopentadienyl.

I.5 Preparation of the ferrocene and its derivatives:

I.5.A Preparing ferrocene:

- The following reaction demonstrates the original preparation of the ferrocene as described by Pauson and Kealy, using Grignard reagents for the two pentadienyl rings [22], Eq.11.

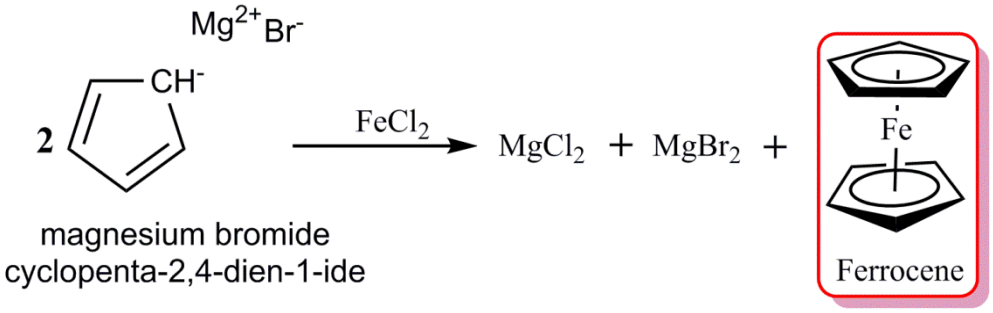

Figure.11. Preparation of the ferrocene as described by Pauson and Kealy.

- One of the simplest and most applicable methods of preparing ferrocene and other metallocenes is by direct mixing of the cyclopentadiene sodium salt with ferrous chloride ($FeCl_2$) in tetrahydrofurane (THF) [23], which is shown in Eq.12.

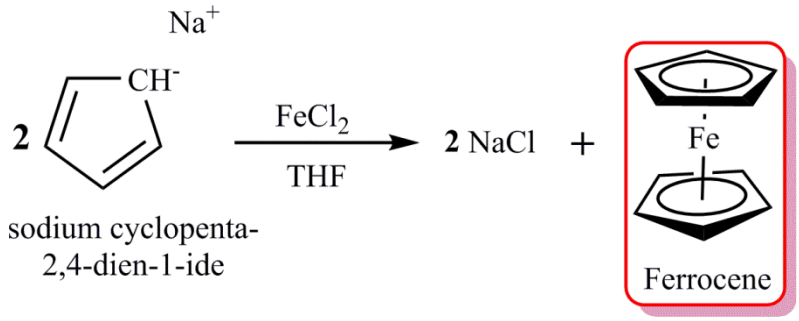

Figure.12. Preparation ferrocene from reacting sodium cyclopentadiene salt with ferrous chloride in tetrahydrofurane medium.

- Direct reaction of dicyclopentadienyl with ferrous chloride in presence of an amine compound [17], Eq.13.

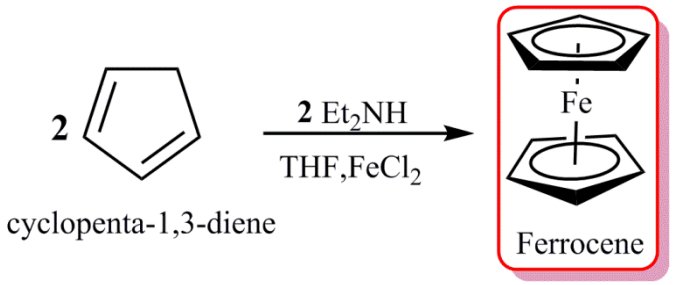

Figure.13. Ferrocene Preparation from reacting sodium cyclopentadiene salt with ferrous chloride in presence amine compound.

I.5.B **Preparing ferrocene derivatives [17]:**

B.a From ferrocene:

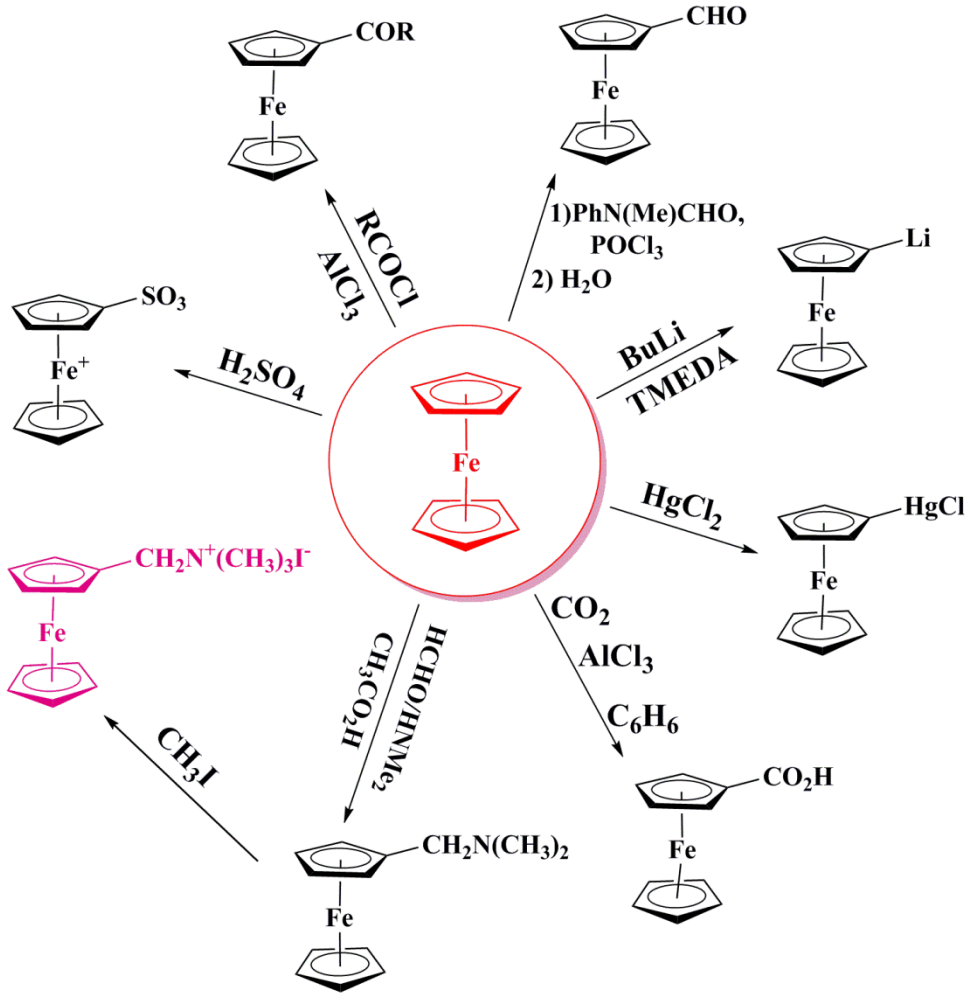

Figure.14. Preparing ferrocene's derivatives from ferrocene.

B.b From ferrocenyl methyltrimethylammonium iodide salt ($C_{14}H_{20}F_eIN$):

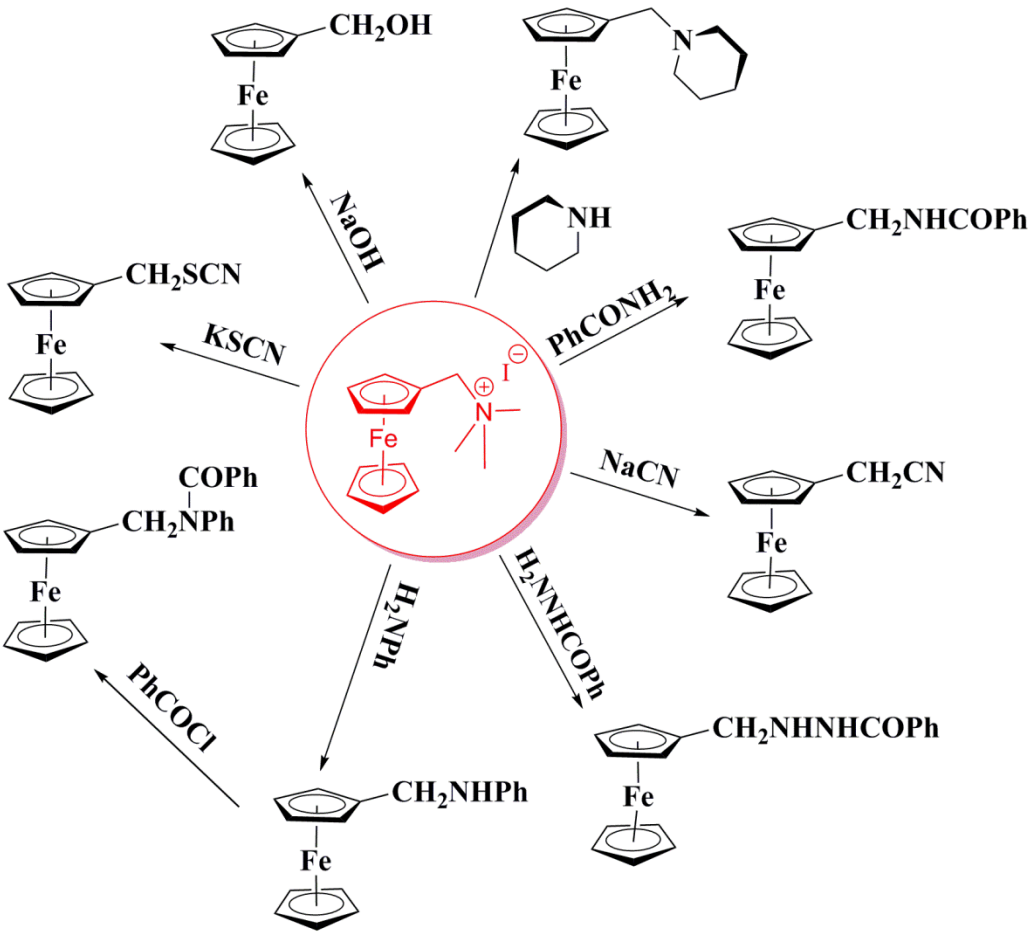

Figure.15. Preparing ferrocene's derivatives from ferrocene salt.

Preparation of the ferrocenyl methyltrimethylammonium iodide salt ($C_{14}H_{20}FeIN$) [24]:

It is preparing from dimethylamine (C_2H_7N) by three steps:

B.b.1 ***First step: Mannish reaction.***

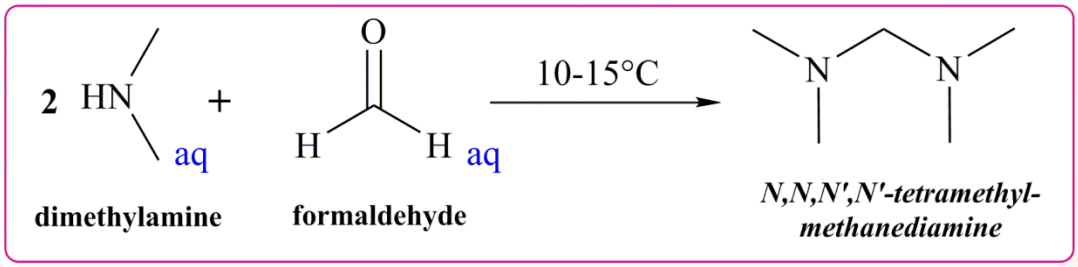

Figure.16. Mannish reaction.

B.b.2 *Second step: preparing N, N-dimethylaminoferrocene (electrophilic substitution).*

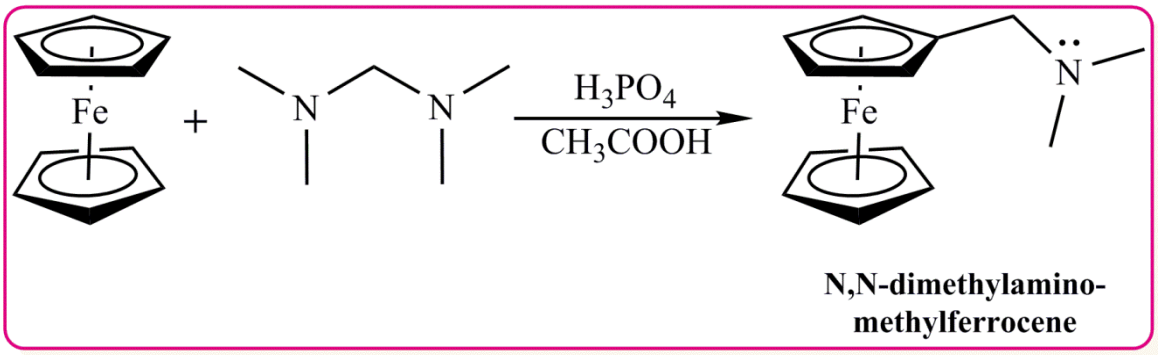

Figure.17. Preparing N, N-dimethylaminoferrocene.

B.b.3 *Third step: ferrocene salt.*

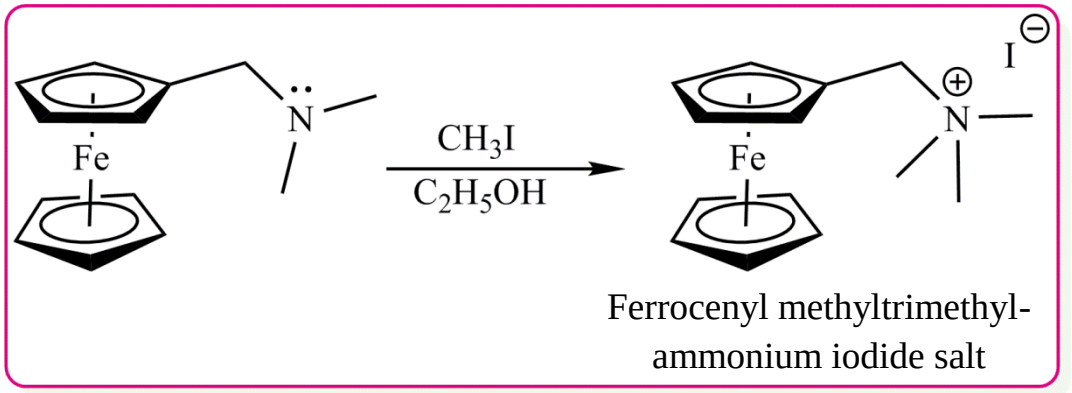

Figure.18. Preparing ferrocenyl methyltrimethylammonium iodide salt ($C_{14}H_{20}F_eIN$).

I.6 Applications of the ferrocene and its derivatives:

I.6.A Fuel additives:

The ferrocene is used in the manufacture of plastics and fuels to reduce smoke in two materials such as polyurethane combustion, and it is used in a ratio ranging between 0.25% and 0.5%, i.e.: N, N-dimethylaminomethyl cyclopentadienyl iron, butyryl dicyclopentadienyl iron, hexadicyl ferrocene [17].

I.6.B Gas Sensors:

Two virus-based polymers are used within optical fiber devices as gas sensors such as explosive gas alarm, hazardous waste analysis and pollution detection [17].

I.6.C Antimalarials:

The disease is caused by the parasite plasmodium falciparum or Plasmodium falciparum, and various treatments have been used against it, such as Chloroquine, but the pathogen has shown

resistance over time, and since the parasite needs iron inside the red blood cells, Brocard and his colleagues, in the end of the 1990s, combined the drug with ferrocene in the same molecule, thus producing a hybrid Ferroquine. It is the one that turned out to be stronger than the previous one [17].

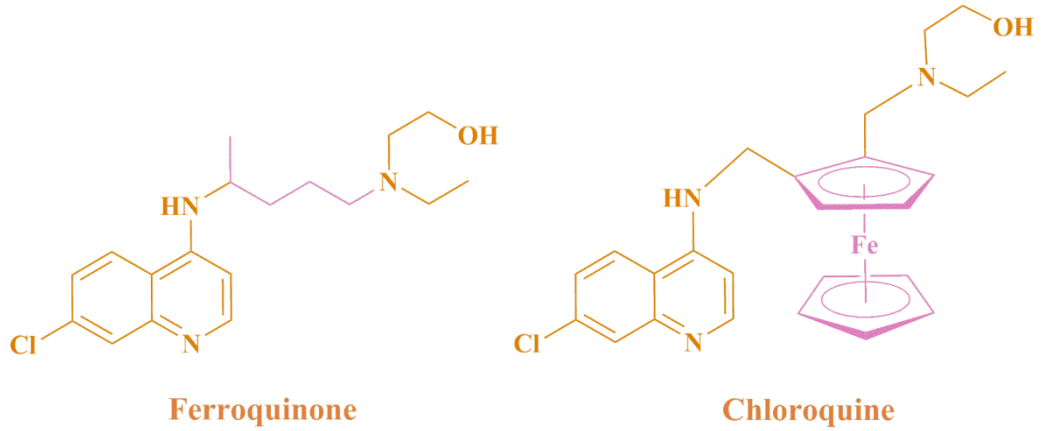

Figure.19. Antimalarials compounds: Ferroquine and Chloroquine.

I.6.D Antibiotics:

In the 1970s, E. I. Edward and a research team designed a series of viral-associated antibiotics that included Ferrocenyl-penicillin, Ferrocenyl-cephalosporin, Ferrocenyl-hybrid of penicillin, and cephalosporin [17].

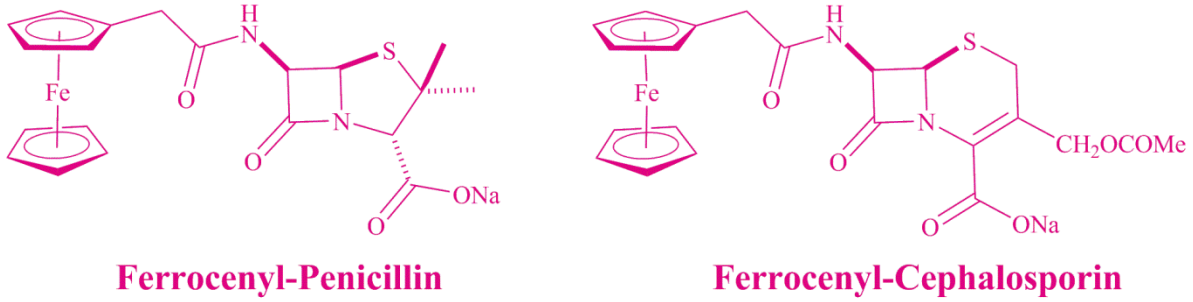

Figure.20. Antibiotics compounds: Ferrocenyl-penicillin and Ferrocenyl-cephalosporin.

I.6.E Corrosion inhibition:

For example, 1,1'-diformylferrocene (Diformyl Fc), 1,1'-diacetylferrocene (Diacetyl Fc), and 2-benzimidazolylthioacetylferrocene (BIM Fc), shown in Fig.21, a, were used as corrosion inhibitors, by studying the impedance and polarization resistance technique (Rp). The inhibitory ability of these compounds was tested in HCl and H_2SO_4 solutions.

Such as sixth ferrocenylmethyl aniline compounds substituted by Nitril ($C \equiv N$) and Nitro (NO_2) groups, shown in Fig.21, b, has been used. The Nitro (NO_2) substituted compounds,

were studded by Rahim, O., et al. [2], using Electrochemical impedance spectroscopy (EIS). Are suggested to discuses and compare with other previous studies.

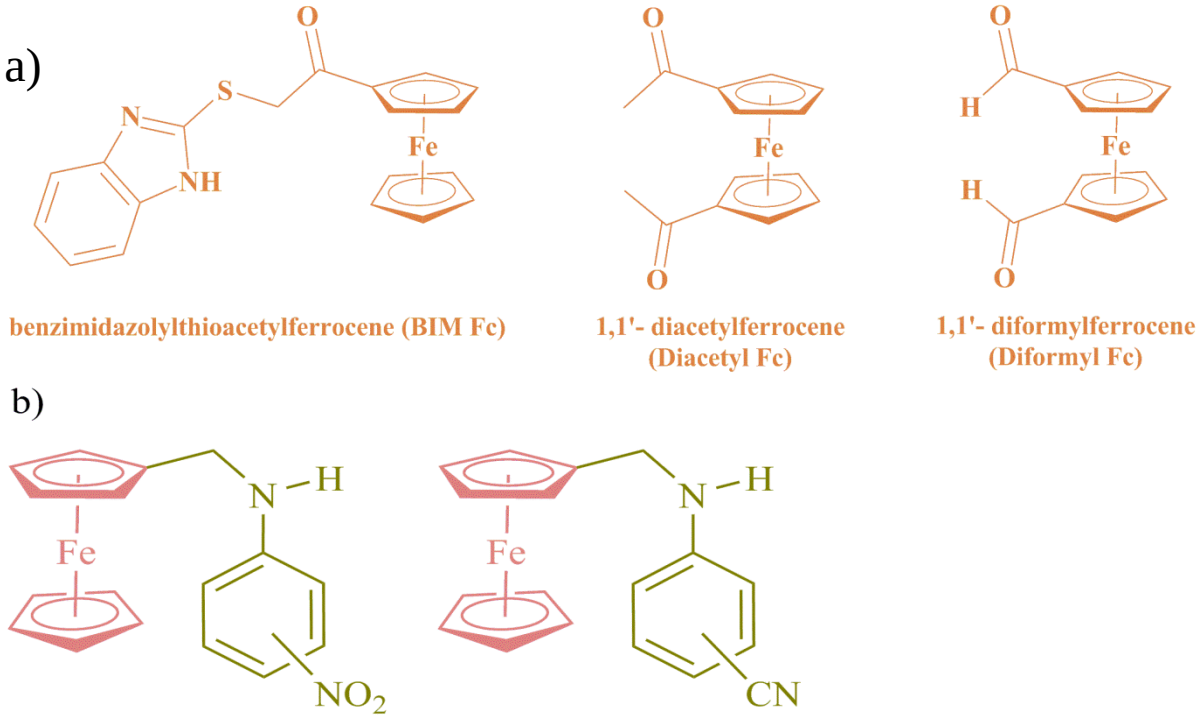

Figure.21. Some Ferrocene derivatives compounds used as corrosion inhibition.

References:

English

1. Werner, H., *At least 60 years of ferrocene: the discovery and rediscovery of the sandwich complexes.* Angewandte Chemie International Edition, 2012. **51**(25): p. 6052-6058.
2. Rahim, O., et al., *Evaluation of the inhibitory effectiveness of three ferrocene derivatives for corrosion of steel XC70 by spectroscopy of electrochemical impedance.* Journal of Fundamental and Applied Sciences, 2011. **3**(2): p. 210-223.
3. Radwan, A.B., et al., *Corrosion inhibition of API X120 steel in a highly aggressive medium using stearamidopropyl dimethylamine.* Journal of Molecular Liquids, 2017. **236**: p. 220-231.
4. Nazir, U., et al., *Biferrocenyl Schiff bases as efficient corrosion inhibitors for an aluminium alloy in HCl solution: a combined experimental and theoretical study.* RSC Advances, 2020. **10**(13): p. 7585-7599.
5. Sayed, A.R. and H.M.A. El-Lateef, *Thiocarbohydrazones Based on Adamantane and Ferrocene as Efficient Corrosion Inhibitors for Hydrochloric Acid Pickling of C-Steel.* Coatings, 2020. **10**(11): p. 1068.
6. Fatima, S., et al., *Study of new amphiphiles based on ferrocene containing thioureas as efficient corrosion inhibitors: Gravimetric, electrochemical, SEM and DFT studies.* Journal of Industrial and Engineering Chemistry, 2019. **76**: p. 374-387.
7. Verma, C., M. Quraishi, and A. Singh, *A thermodynamical, electrochemical, theoretical and surface investigation of diheteroaryl thioethers as effective corrosion inhibitors for mild steel in 1 M HCl.* Journal of the Taiwan Institute of Chemical Engineers, 2016. **58**: p. 127-140.
8. Morad, M. and A. Sarhan, *Application of some ferrocene derivatives in the field of corrosion inhibition.* Corrosion Science, 2008. **50**(3): p. 744-753.
9. Gupta, S.R., et al., *Synthesis, structural, electrochemical and corrosion inhibition properties of two new ferrocene Schiff bases derived from hydrazides.* Journal of Organometallic Chemistry, 2014. **767**: p. 136-143.
10. Miller, S.A., J.A. Tebboth, and J.F. Tremaine, *114. Di cyclo pentadienyliron.* Journal of the Chemical Society (Resumed), 1952: p. 632-635.
11. Kealy, T. and P. Pauson, *A new type of organo-iron compound.* Nature, 1951. **168**(4285): p. 1039-1040.
12. Pauson, P.L., *Ferrocene-how it all began.* Journal of Organometallic Chemistry, 2001. **637**: p. 3-6.
13. Kavallieratos, K., S. Hwang, and R.H. Crabtree, *Aminoferrocene derivatives in chloride recognition and electrochemical sensing.* Inorganic chemistry, 1999. **38**(22): p. 5184-5186.

14. Wilkinson, G., et al., *Ferrocene.* J. Am. Chem. Soc, 1952. **74**: p. 1-10.

15. Eiland, P.F. and R. Pepinsky, *X-ray examination of iron biscyclopentadienyl.* Journal of the American Chemical Society, 1952. **74**(19): p. 4971-4971.

16. Seiler, P. and J. Dunitz, *Low-temperature crystallization of orthorhombic ferrocene: structure analysis at 98 K.* Acta Crystallographica Section B: Structural Crystallography and Crystal Chemistry, 1982. **38**(6): p. 1741-1745.

18. Dagani, R., *Fifty years of ferrocene chemistry.* Chemical & Engineering News, 2001. **79**(49): p. 37-37.

19. Khelef, A., *Synthèse et étude du comportement anodique de quelques N-ferrocenyl-N-phenylalkanamides et N'-ferrocenyl-N'-phenylalkanehydrazides et étude structurale de leurs phases cristallines*. 2014, Université Mohamed Khider Biskra.

20. Terki, B., *Synthèse, cycliisatiion, étude électrochimique et structurale de quelques n--acyl--n''alkylférrocenyl méthyle hydrazide*. 2007, Batna, Université El Hadj Lakhdar. Faculté des sciences.

21. Biot, C., *Molécules ferrocéniques antipaludiques: synthèse, caractérisation et activité*. 1998, Lille 1.

22. Rausch, M., M. Vogel, and H. Rosenberg, *Ferrocene: a novel organometallic compound.* Journal of Chemical Education, 1957. **34**(6): p. 268.

23. Salinger, R., *Survey of Progress in Chemistry.* AF de Scott, 1963. **1**: p. 301.

24. TERKI, B. and T. LANEZ, *ANODIC BEHAVIOUR INVESTIGATION OF (FERROCENYLMETHYL) TRIMETHYLAMMONIUM CATION.*

Arabic:

17. رحيم ، أ. التصنيع والدراسة الإلكتروكميائية والبنيوية لبعض مستبدلات *N*-فيروسينيل ميثيل الأنيلين وتطبيقها في تثبيط التآكل المائي. 2014، اطروحة دكتوراه، جامعة قاصدي مرباح- ورقلة، الجزائر.

Second chapter:

Electrochemical Impedance Spectroscopy (EIS)

II.1 Introduction:

Corrosion is the deterioration of metal by chemical action or a reaction with the environment. It is a regular and continuous problem, often difficult to remove completely. The corrosion of mild steel and other metals is rigorous in the presence of an aggressive medium such as acid. Therefore industrial process such as acid cleaning, acid descaling, acid pickling, and other oil well acidizing processes, requires the use of corrosion inhibitors [1].

Most investigated organic compounds that used as an inhibitor are toxic and cause severe environmental hazards, therefore their replacement by environmentally benign inhibitors is necessary [2].

Interest in ferrocene-based compounds has immensely increased owing to their favorable electronic properties, ease of functionalization and exceptional stability towards water and air [3], and have favorable electrochemical properties [4].

Numerous chemical properties have made ferrocene a striking molecule in a variety of applications. They have promising electrochemical properties and are usually non-toxic [5].

Application of corrosion inhibitors is the most economical and practical method to mitigate electrochemical corrosion [6]. Electrochemical Impedance spectroscopy (EIS) is used to study the corrosion behavior at the metal solution interface.

In this chapter, three of new derivatives compounds of ferrocenyl amines inhibitors, Fc-1, Fc-2 and Fc-3 are studied electrochemically as inhibitions of corrosion in acidic medium with Electrochemical Impedance spectroscopy (EIS) and discussed some of their electrochemical properties such as double layer capacitance (C_{dl}), and charge transfer resistance (R_{ct}), and compared with some previous studies.

II.2 Materials and Methods [7]:

II.2.A **Chemicals that used:**

Table.1. Chemicals that used.

	Chemical formula	**Purification degree (%)**	**Molar mass (g/mol)**	**Density (g/ml)**	**Company production**
Hydrochloric acid	HCl	37	35.5	1.18	Merck
Acetone	CH_3COCH_3	Pure	46	/	Merck
Methanol	CH_3OH	98	32	0.645-0.665	Merck
Distillated water	H_2O	/	18	1	/

II.2.B **Composition of steel (XC70) specimen:**

Carbon steel XC70 is widely uses in petroleum and gas industry, refinery units, pipelines, chemicals, and oil gas production units, which released from pipelines factory in Ghardaia.

Table.2. Chemical components of carbon steel specimen (XC70).

Elements	**C**	**P**	**S**	**Si**	**Mn**	**Cr**	**Ni**	**Cu**	**Al**	**Nb**	**V**	**Ti**	**Mo**	**Fe**
Value % ($\times 10^{-3}$)	**65**	**2**	**1**	**245**	**1685**	**42**	**26**	**10**	**42**	**67**	**14**	**19**	**5**	**Rest**

II.2.C **Electrochemical measurements:**

It is used to understand the fundamental mechanism of corrosion inhibition in the metals.

Electrochemical measurements were performed using a personal computer-driven Volta lab 40 model PGZ301 Potentiostat state quipped with Volta Master 4 software.

A typical three electrodes cell with a reference electrode represented by a saturated calomel electrode (SCE), the auxiliary electrode was a platinum plate (1 cm^2) and the working electrode made of carbon steel (XC70) with an active surface of (1 cm^2) which was polished until 4000 grade emery paper, degreased with acetone, rinsed with deionizer water and air-dried.

Electrochemical impedance spectroscopy (EIS) measurements were carried out after 20 minutes immersion time of the carbon steel specimen in corrosive media, at the corrosion potential E_{corr} = -479 mV with a frequency ranging from 20KHz to 40mHz with 10mv amplitude of sinusoidal wave, the immersion time is 20 minutes, and 4 minutes of stabilization before reading, at room temperature 25°C.

The aim of this work is electrochemical studying a new ferrocenyl amines derivatives as inhibitions of corrosion in acidic medium, they are: Fc-1, Fc-2 and Fc-3, shown in Fig.22.

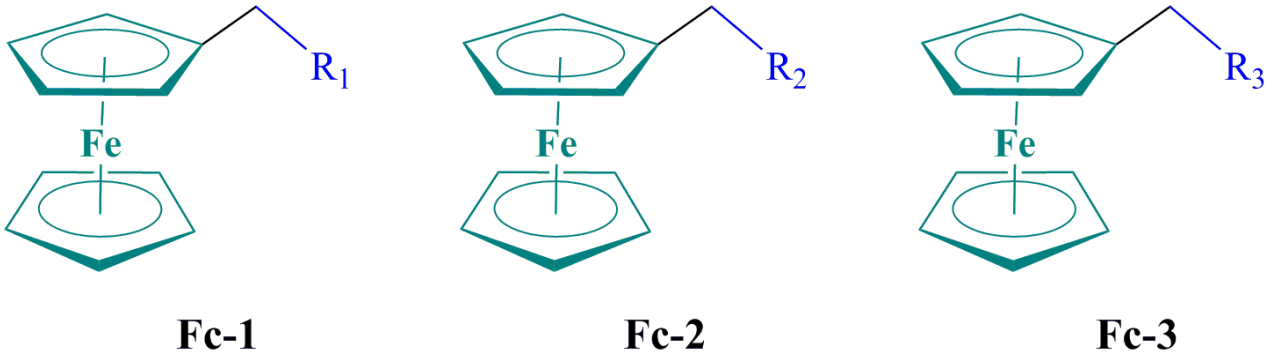

Figure.22. ferrocenyl amine derivatives that are being studied.

Becouse of compounds are poor soluble on acidic solution they dissolved in 15% methanol.

Corrosive medium is solution of hydrochloric acid (HCl) 1M, prepared from concentrated acid and distillated water. Solutions of ferrocene derivatives (10–80 ppm) were prepared by dissolving the required weight in methanol (Merck).

II.3 Results and discussion

II.3.A **Electrochemical impedance spectroscopy (EIS):**

EIS is a powerful technique that used to study electrode/electrolyte interface. This technique has been used to understand different localized corrosion reactions and estimate their rate[8]. EIS data were analyze and fitted using the equivalent electrical circuit (EEC), known as simplified Randles circuit, for metal/electrolyte interface, shown in Fig.23.

Fig.24 shows Nyquist plots (upper), Bode plots (middle) and phase angle plots (lower) for the XC70 in 1M HCl without and with 10-80ppm of Fc-1 (a), Fc-2 (b) and Fc-3 (c) obtained within frequency range 20 kHz to 40 Hz.

Nyquist plots (Z_{Real} vs.Z_{imag}) Fig.24, upper, shows a depressed capacitive loop which arises from the time constant of the electrical double layer (C_{dl}) and charge transfer resistance (R_{ct}). The semicircle indicated the formation of a protective layer of the ferrocenyl amine derivatives on the specimen surface. Therefore, the charge transfer resistance associated with the corrosion activity and the behaviors of the electrical double layer are elucidated [9]. Fig.25, 26 and 27, shows R_{ct}, C_{dl} and IE% values recorded by EIS, reveals that they are flow oscillatory pattern, which indicted for all inhibitors. Nyquist plots of all inhibitors exhibited increasing the capacitive loop radius with increasing the inhibitor's concentration which leads to decreasing double layer capacitance and increasing charge transfer resistance and consequently the inhibition efficiency increases, summarized in Table.3.

Analysis of Nyquist plot reveal that is a depressed semicircle and that ascribed to the frequency scattering as a result of different physical phenomena such as non-homogeneity surfaces of solid, roughness of the substrate surface, mass transport process, distribution of the surface active sites and the resulting adsorption process.

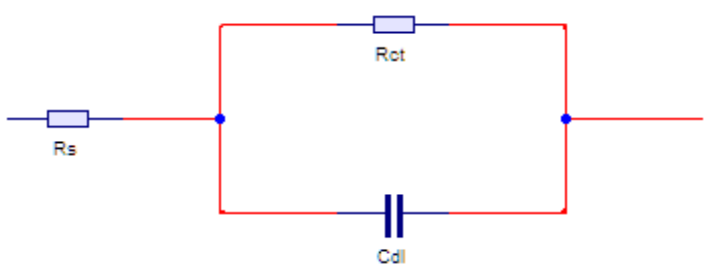

It is equal to:

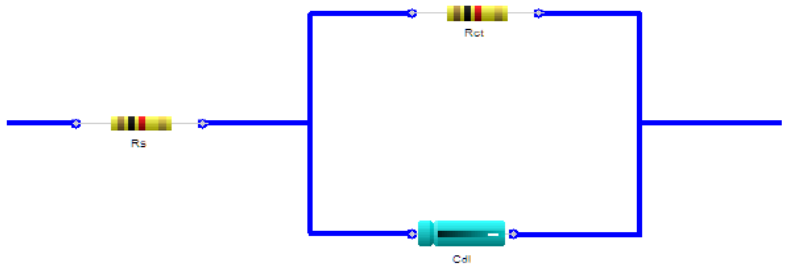

Figure.23. the equivalent electrical circuit (EEC) of the XC70 steel in 1M HCl at effective concentration of Fc-1, Fc-2and Fc-3.

80ppm of Fc12, Fc13and Fc14 obtained at E_{corr}, is assessed by Eq.1 [10]:

$$Z = R_s + \frac{R_{ct}}{1+j\omega R_{ct}C_{dl}} \quad (1)$$

Note that $R_s$is solution resistance, j is equal to $\sqrt{-1}$ contrary to IUPAC convention to not be confused with current, ω is in unit s^{-1} which equal to $2\pi f$.

Table.3. Summary of electrochemical impedance spectroscopy (EIS) parameters of the XC70 steel in 1M HCl at effective concentration of Fc-1, Fc-2 and Fc-3, which IE % calculated according to R_{ct} values.

Table.3. Summary of electrochemical impedance spectroscopy (EIS) parameters of XC70 steel in 1M HCl at effective concentration.

	C (ppm)	C (mol/l)	R_{ct} (ohm.cm²)	C_{dl} (µF.cm-²)	f_{Max} (Hz)	IE %	θ
HCl	/	/	45.987	276.549	31.646	/	/
Blank	/	/	46.693	278.803	31.646	/	/
Fc-12	70	2.08E-04	533.122	157.907	5.000	91.374	0.914
Fc-13	80	2.38E-04	332.987	162.954	7.937	86.190	0.862
Fc-14	70	2.08E-04	424.643	84.674	10.218	89.170	0.892

R_{ct}: Charge transfer resistance, C_{dl}: capacity electric of the double layer, f_{Max}: frequency value at maximal impedance imaginary component, which is calculated using R_{ct} and C_{dl} values and according to the following Eq.2:

$$f_{Max} = f_{-iz_{Max}} = \frac{1}{2\pi R_{ct}C_{dl}} \quad (2)$$

IE%: Inhibition efficiency which is calculated using R_{ct} values according to the following Eq.3:

$$IE\% = \left(1 - \frac{R_{ct}^{0}}{R_{ct}}\right) \times 100 \quad (3)$$

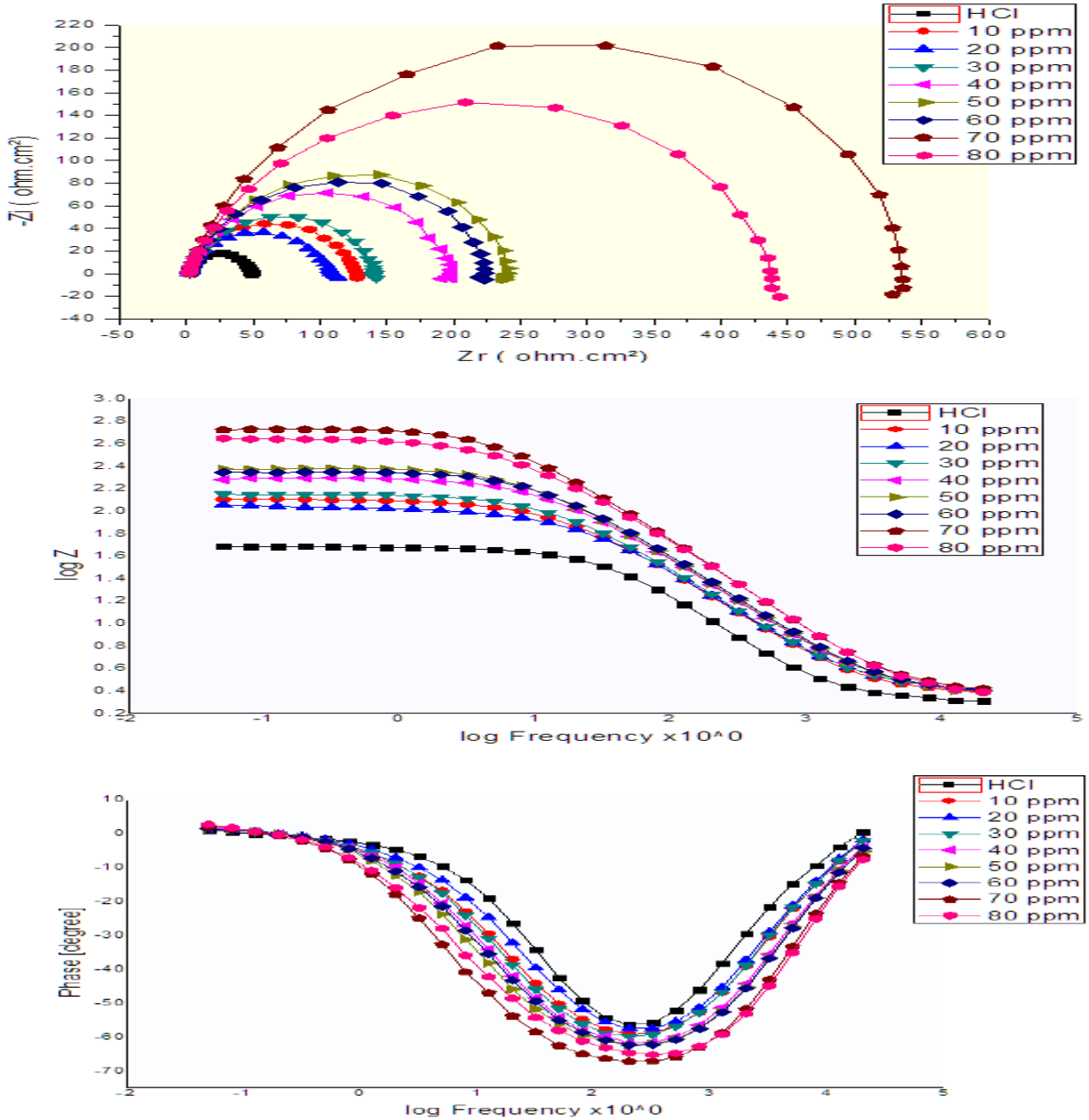

Figure.24.a. Nyquist (upper), Bode (middle) and phase angle plot (lower) without and with 10-80ppm of Fc-1.

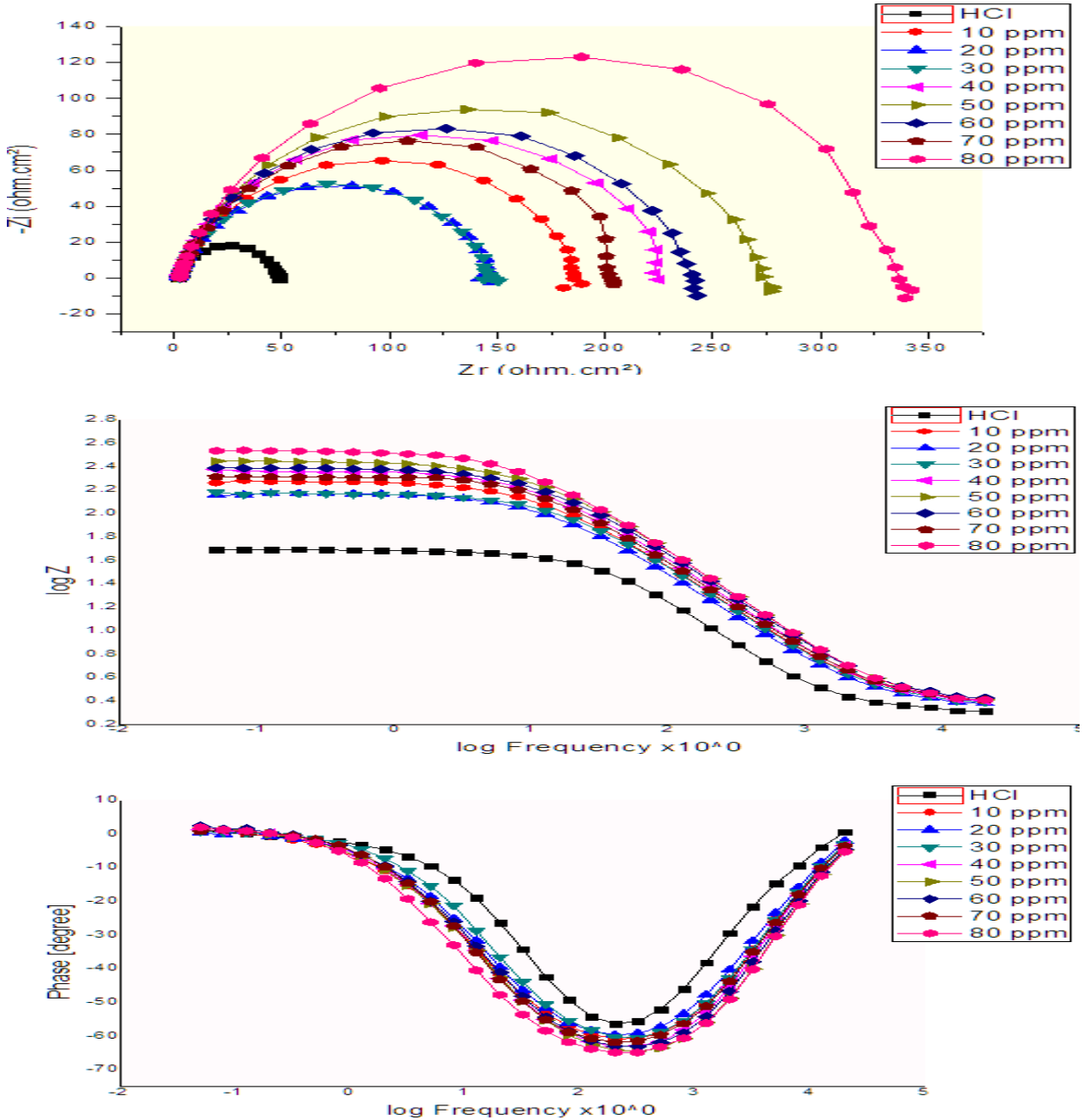

Figure.24.b. Nyquist (upper), Bode (middle) and phase angle plot (lower) without and with 10-80ppm of Fc-2.

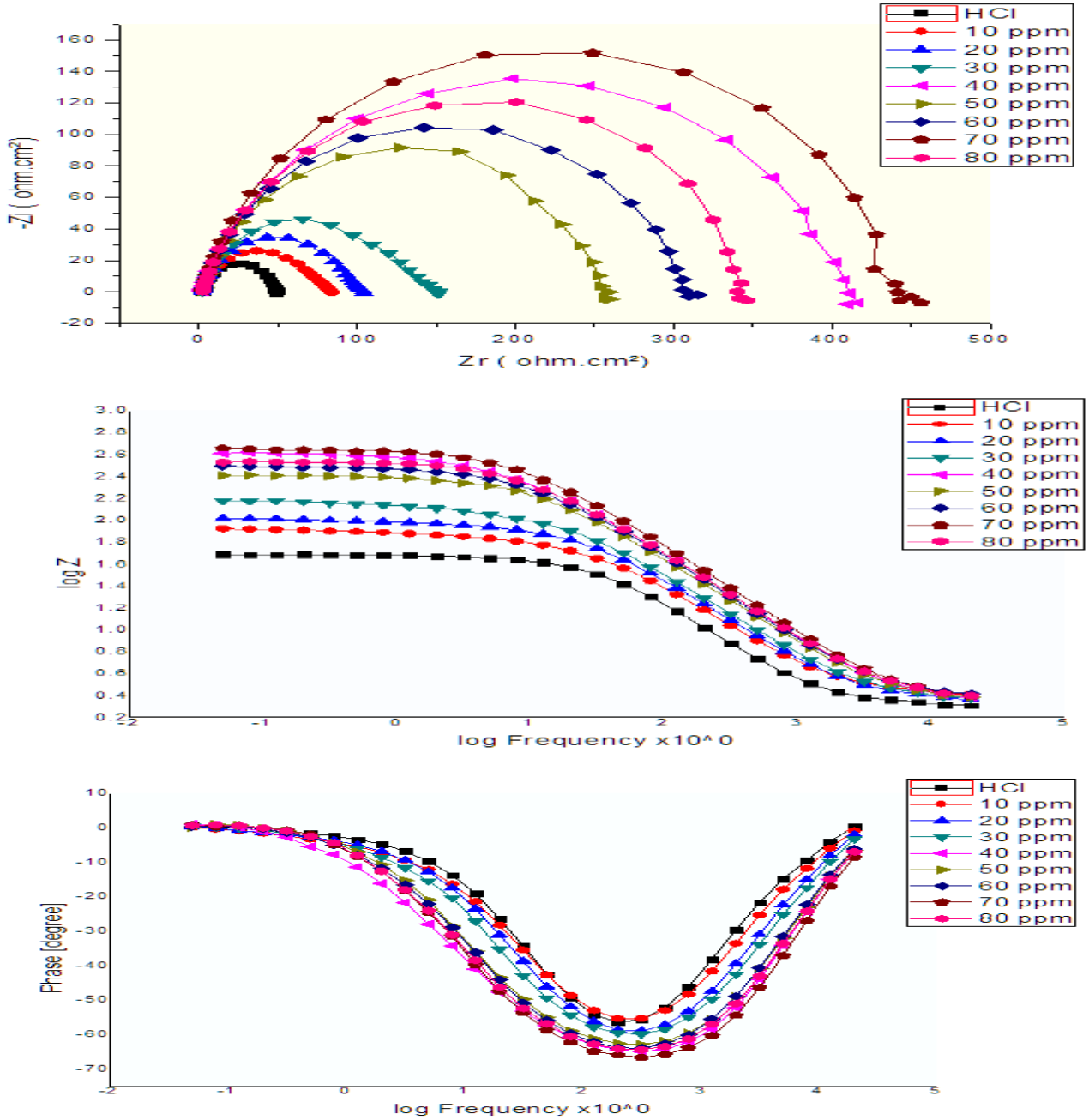

Figure.24.c. Nyquist (upper), Bode (middle) and phase angle plot (lower) without and with 10-80ppm of Fc-3.

Where R_{ct}^{0} and C_{dl}^{0} are the charge transfer resistance and double-layer capacitance respectively in the blank solution.

θ: Surface coverage, which is calculated according to the following Eq.4:

$$\theta = \left(1 - \frac{R_{ct}^{0}}{R_{ct}}\right) \quad (4)$$

A.a **Discussion Nyquist plot:**

The asymptotic limits of the real part of impedance for the reactive circuit of Fig.24, upper, are $R_e$at high frequencies and $R_e + R_{ct}$ at low frequencies were the negative imaginary impedance reaches a maximum value is equal to $\frac{R_{ct}}{2}$ for a single RC circuit.

A.a.1 **Discussion of the charge transfer resistance (R_{ct}):**

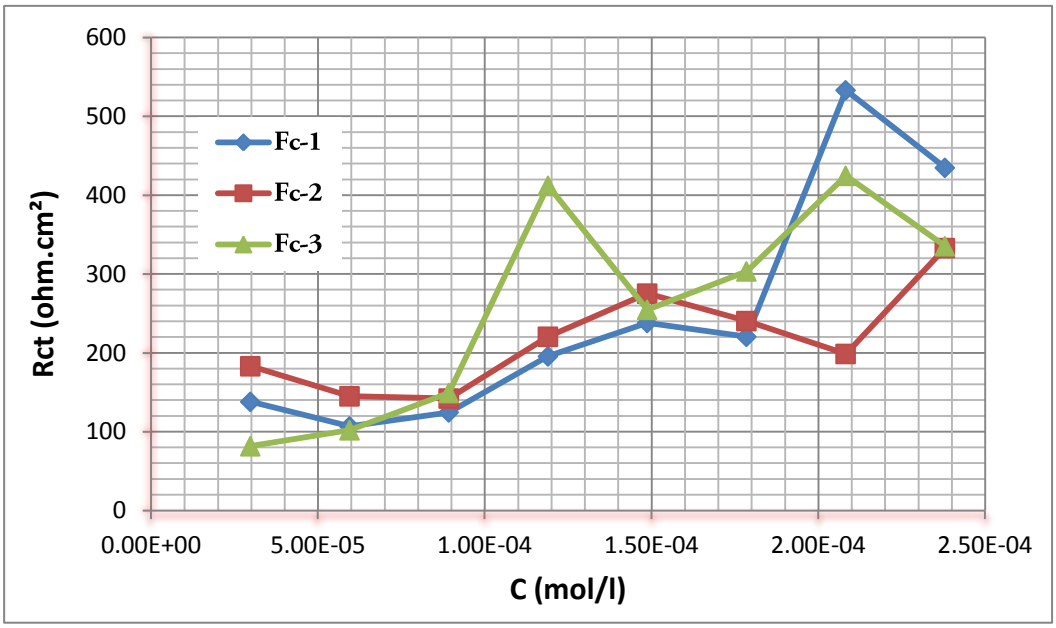

Figure.25. variation of solution resistance (R_{ct}) versus concentration of inhibitors.

As shown in Table.3, the charge transfer resistance of the HCl and blank solutions were estimated at *45.987 ohm.cm²*, *46.693 ohm.cm²*, which increase in presence of different inhibitors, the R_{ct} value of Blank solution is higher than HCl solution, that means it has low corrosive rate of steel specimen, that due to OH group of methanol and its free pairs of electrons, which assesses to form barrier layer. At effective concentration of each compound, R_{ct} of Fc-1, Fc-2 and Fc-3 are found to be *533.122 ohm.cm²*, *332.987 ohm.cm²*, and *424.643 ohm.cm²*, in order, as shown in Fig.25. The high charge transfer resistance value of Fc-1 can be attributed to ascending tendency of inhibitor to form an adsorbed protective layer on to the metal surface, thereby deactivating the inhibition process [5, 11], and

also may be attributed to the blocking of active site of metal surface by surface adsorption and increase inhibition efficiency, unlike Fc-3 and Fc-2 who have low R_{ct} values.

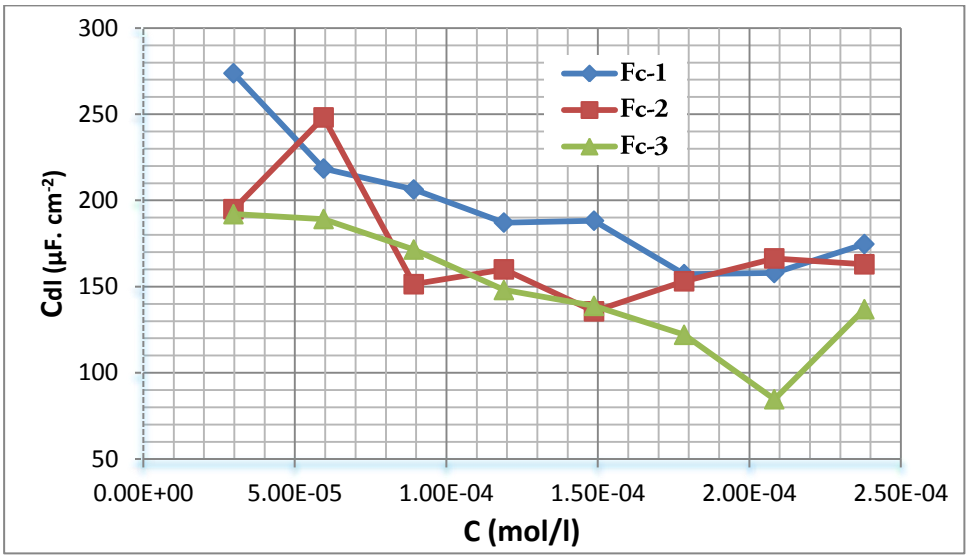

Figure.26. variation of double layer capacitance (C_{dl}) versus concentration of inhibitors.

A.a.2 Discussion of the double layer capacitance (C_{dl}):

The blank solution has highest capacitance value *(276.540 µF /cm²)* than HCl's value *(278.803 µF/cm²)*, which decrease in the presence of different inhibitors at effective concentration (Table.3), C_{dl} value of Blank solution is higher than HCl solution, may refer to high dielectric constant of methanol molecules, precisely oxygen atoms, and an increase in electric double layer. The Fc-14 inhibitor has lowest capacitance value (*84.674 µF/cm²*) compare to Fc-1 and Fc-2 (*157.907 µF/cm²* and *162.950 µF/cm²* in order), shown in Fig.26 that can be attributed to Fc-3 inhibitor shows ascending tendency to decrease in electric double layer, which is more likely due to the replacement of water molecules having higher dielectric constant with the inhibitor molecules possessing lower dielectric constant and /or an increase in the thickness of electric double layer. This finding further suggests the formation of protective film of Fc-3 on mild steel surface [5, 6, 12].

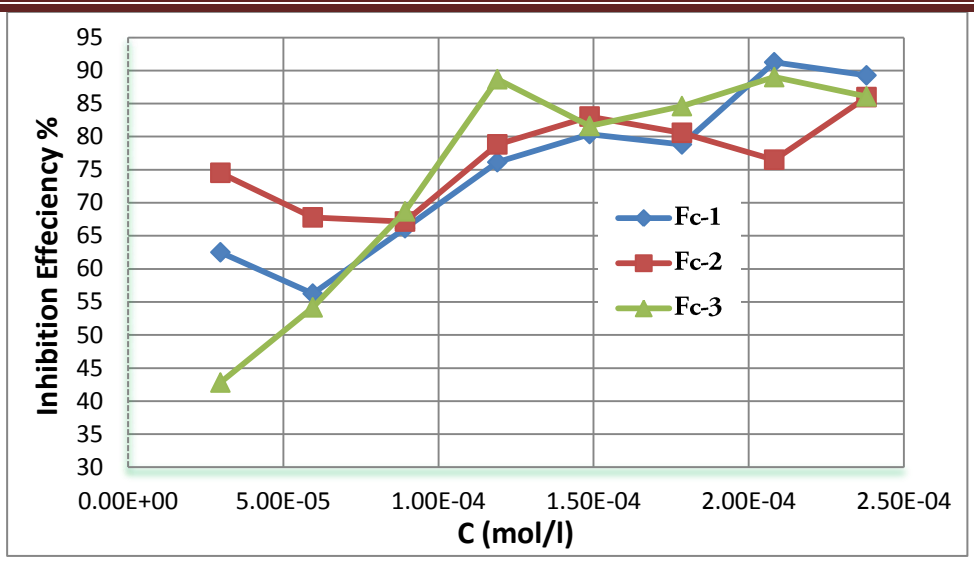

Figure.27. inhibition efficiency (IE %) of inhibitors versus concentration of inhibitors.

A.a.3 **Discussion of the inhibition efficiency of inhibitors (IE %):**

Noted that the IE % values of Fc-1 and Fc-2 inhibitors are fluctuating (Fig.27), they do not show a clear linear relation, as they decrease, then increase, and then return to decrease with an increase in the concentration if inhibitors. Inhibitor Fc-3 shows a direct relationship with the increase in the concentration, except for fifth and last of concentration values. The highest IE % value for Fc-1 inhibitor was ***91.24%***, recorded at concentration ***70ppm***, and for Fc-3 inhibitor, scored ***88.67%* at *70ppm***, while the Fc-2 inhibitor exhibit high IE % **(*85.97%*)** at concentration ***80ppm***, shown in Table.3.

Conclude that, the Fc-1 inhibitor has highest IE % value, followed by Fc-3 inhibitor, and Fc-2 inhibitor shown lowest IE % value. Nevertheless, Fc-2 inhibitor is the best economically inhibitor with ***74.52%*** at ***10ppm***, that attributed to low concentration with high inhibition efficiency.

A.b **Discussion Bode plot:**

The Bode plots Fig.24. Middle; demonstrating the variation of impedance vs. logarithm of frequency ($Log\ f$ vs. $Log\ Z$), indicate the increase in R_{ct} with the increase in inhibitor concentration. Eq.5 represents the mathematical expression of impedance magnitude.

$$|Z| = \sqrt{Z_{Re}^2 + Z_{Im}^2} \quad (5)$$

Which:

$$Z_{Re} = R_s + \frac{R_{ct}}{1+(\omega R_{ct} C_{dl})^2} \quad (6)$$

$$Z_{Im} = -\frac{j\omega C_{dl} R_{ct}^2}{1+(\omega R_{ct} C_{dl})^2} \quad (7)$$

High frequency impedance and phase angle ($Log\ f$ vs.Φ), revealed the heterogeneities and roughness of metal surface [13, 14], shown in Fig.24. Lower. The mathematical expression of phase angle represents in Eq.8.

$$\Phi = \tan^{-1}\left(\frac{Z_{Im}}{Z_{Re}}\right) \quad (8)$$

The phase angle tends to toward -90 at low frequencies, and toward zero at high frequencies, which the phase angle tends to toward 0 for resistor and tends to toward +90 for inductor and tends to toward -90 for capacitor [10].

It is obvious that from the Bode plot the impedance magnitude (S) and phase angle (Φ) fall to zero at high frequency region. However , the transition between low frequency and high frequency for bode plot asymptotes has a slope values close to unity and the phase angle values ranges in between –55.37° and –67.17° have been observed.

Table.4. Bode plot data of impedance magnitude slope (S) and angular phase (Φ).

C (ppm)	Bode plot					
10	-0.6961	-59.12	-0.7169	-60.89	-0.6602	-55.37
20	-0.6843	-57.49	-0.7028	-59.76	-0.6968	-58.93
30	-0.7036	-59.86	-0.7175	-60.59	-0.7056	-59.88
40	-0.7262	-61.69	-0.746	-63.12	-0.7591	-64.92
50	-0.7301	-62.4	-0.7604	-64.61	-0.7362	-62.9
60	-0.735	-62.33	-0.7456	-63.2	-0.7509	-63.99
70	-0.7821	-67.17	-0.7275	-61.95	-0.7771	-66.66
80	-0.7624	-65.22	-0.7623	-64.96	-0.753	-64.42
	Slope (S)	Angle (Φ)	Slope (S)	Angle (Φ)	Slope (S)	Angle (Φ)
	Fc-1		Fc-2		Fc-3	

Table.5. List of various synthesizes inhibitors those studied their inhibition efficiency on various metals surface by EIS in HCl and H_2SO_4 medium.

Num	Inhibitors	Metal	Medium	Method	Results				References
					Electrochemical impedance spectroscopy				
						R_{ct} (ohm.cm²)	C_{dl}(µF.cm-²)	IE%	
1	Diacetyl Fc, Diacetyl Fc & BIM Fc	Mild steel	0.5 M H_2SO_4 and 1 M HCl	EIS	Blank	18.9	430	/	[3]
					BIM Fc	119.5	190	84.2	
					➢ **Weak inhibitors in HCl.** ➢ **100µM at 30°C in 0.5 M H_2SO_4 .**				
2	Fc-ph & Fc-fh	Mild steel	0.1 M H_2SO_4	EIS	Blank	9.8	126	/	[15]
					Fc-ph	73.4	76	86.5	
					Fc-fh	110.4	71	91.1	
					➢ **100ppm at 25°C.**				
3	M-11, M-13, M-17	Mild carbon steel (MCS)	1 M HCl	EIS	Blank	15.55 ±0.28	1318 ±22	/	[16]
					M-11	280.8 ±3.55	292 ±13	94	
					M-13	325.5 ±6.36	137 ±6	95	
					M-16	529.1 ±7.20	210 ±9	96	
					➢ **1mM at 60°C.**				
4	Fcua, Fcub & Fcuc	aluminum alloy AA2219-T7	0.1 M HCl	EIS	Blank	128.6	132.2	/	[17]
					Fcua	1630	418.6	92.11	
					Fcub	2390	411.0	94.61	
					Fcuc	3198	217.2	95.97	

					➢ **100ppm at 25°C.**				
5	Fc-Th	Carbon steel	1 M HCl	EIS	Blank	18.7 ±2	336.1	/	[18]
					Fc-Th	464.1 ±33	39.6	95.9	
					➢ **200ppm at 50°C**				
6	Fc-1, Fc-2 & Fc-3	XC70 carbon steel	1 M HCl	EIS	Blank	45.987	276.549	/	[7]
					Fc-1	533.122	157.907	91.24	
					Fc-2	332.987	162.954	85.97	
					Fc-3	424.6428	84.6735	89	
					➢ **At 25°C.** ➢ **70ppm for Fc-3 and Fc-1.** ➢ **80ppm for Fc-2.**				

EIS – Electrochemical impedance spectroscopy, WLS – Weight loss study, PDP – Potentio-dynamic polarization.

Increasing the width of the phase angle curves as concentration of inhibitors increase, reveals lower corrosion rates at higher concentration of ferrocenyl Schiff bases inhibitors, which is mainly attributed to increase in the double layer thickness and reduction the local dielectric constant.

II.4 Conclusion:

The inhibition efficiency and the method performance based on ferrocene containing NO_2 group in different positions have been compared with previously reported ferrocene based inhibitors as shown in Table.5.

The comparation Fc-12 inhibitor with compounds consists of ferrocene moiety that synthesized and studded corrosion inhibition on mild steel in 1M HCl solution at different temperature and concentration.

The inhibitor 4,4'-((((ethane-1,2-diylbis(oxy))bis(2-ethoxy-1,4-phenylene))bis(methaneylylidene)) bis(azaneylylidene))bisferrocene (Fcuc) which was studied by Uzma N et al.[17], indicate high charge transfer resistance found to be $3198\ ohm.cm^2$, while ferrocene derivative (octadecanoyl)-3-(4-ferrocenyl-2-methylbenzyl) thiourea (M-17) which was synthesized and studded by S. Fatima et al.[16], its R_{ct} found to be $521.89 - 536.31\ ohm.cm^2$, which is close to Fc-1's R_{ct} $533.122\ ohm.cm^2$, while 2-(ferrocenyl-1-ylidene) hydrazinecarbothiohydrazide Fc-Th inhibitor's R_{ct} is $431.1 - 497.1\ ohm.cm^2$ who synthesized and studied by Abdelwahed R. S et al. [18], suggest that Fcuc molecule has more tendency to form an adsorbed protective layer on the metal surface, high resistance due to increase the thickness of double layer, which decrease in the capacity. Nevertheless M-17, Fcuc and Fc-1 inhibitors shows high double layer capacitance values are $217.2\ \mu F.cm^{-2}$, $201 - 219\ \mu F.cm^{-2}$ and $157.907\ \mu F.cm^{-2}$ respectively, while Fc-Th record low value $39.6\ \mu F.cm^{-2}$, which reveal that Fc-Th inhibitor has more ability to replacement the pre-adsorbed water molecules (H_2O), having higher dielectric constant, with inhibitor molecules leading to the development of a defensive film on the metal interface. This causes a lowering of the local dielectric constant and also a thickening of the double layer. These two aspects cause an enhancement in the capacitive performance and the part of surface coverage (θ), which assessed using Eq.4, by effective adsorption of inhibitor molecules, which led to improving the protection capacity.

The inhibition efficiency (IE %), which assessed using Eq.3, of M-17, Fcuc, Fc-Th and Fc-1 inhibitors are *97 %*, *95.97 %*, *95.90 %* and *91.24 %*, respectively. Fcuc and M-17 inhibitors clearly are much better as an inhibitor in 1M HCl solution, that could be described by two sides, first side may be refer to the concentration of M-17 inhibitors are used $10^{-3}M$ and Fc-Th, Fc-1 and Fcuc inhibitor $6.32 \times 10^{-4}\ M$, $2.08 \times 10^{-4}M$ and, $1.14 \times 10^{-4}\ M$ at high concentration could find a large

number of inhibitor molecules at just small area of steel, which demonstrates the better surface coverage, so at high temperature, M-17 at *60°C* and Fc-Th at *50°C* and at *25°C* for Fc-1 and Fcuc, lead to boost adsorption process rate by increase the electro-activity of inhibitor's molecules, that is increase the adsorption process and enhance the inhibition of corrosion.

The conflicts of R_{ct} , C_{dl} and IE% values might be attributed to steel specimen kind that used in the study, S. Fatima et al. [21], uses Mild carbon steel (MCS), Abdelwahed R. S et al. [22], uses Carbon steel and XC70 steel which used in this study and Uzma N et al. [52], uses aluminum alloy AA2219-T7 the corrosion rate of these specimens in 1M HCl without inhibitors or in the blank solution are $15.27-15.83\ ohm.cm^2$, $16.7-20.7\ ohm.cm^2$, $45.99\ ohm.cm^2$ and $128.60\ ohm.cm^2$ which represented by charge transfer resistance. Obviously that the Mild carbon steel (MCS) has high corrosion rate related to low value of R_{ct} which has direct effect on inhibition efficiency of inhibition.

The comparation the EIS parameters of Fc-1 inhibitor with those of S.R. Gupta et al. [15], who studied the effect of ferrocene carboxaldehyde furoylhydrazone (fcfh) and 2-benzimidazolylthioacetyl-ferrocene (BIM Fc) who synthesized and studded by M.S. Morad, A.A.O. Sarhan [3], on mild steel corrosion in 0.5 M H_2SO_4 solution.

They reveal that the charge transfer resistance R_{ct} of Fcfh and BIM Fc inhibitors are 110.4 ohm.cm² and 119.5 ohm.cm², respectively, much less then Fc-1 inhibitor that has more tendencies to form isolated layer on spaceman surface, may refer to additional benzene ring that consist on nitro aniline moiety who can made more coordination bonds with active sites through donor/acceptor interaction between π -electron and the vacant d orbitals of the iron surface atoms (donation-accepter phenomena). However, non-homogeneity and roughness of the surface, mass transport process and distribution of the surface active sites, all this phenomena could due to crosscut the results, and that indicated in constant phase element (CPE) values, which found to be 71 $\mu\Omega.S^n/cm^2$, 190 $\mu\Omega.S^n/cm^2$ for Fcfh and BIM Fc respectively and double layer capacitance (C_{dl}) of Fc-1 is $157.907\ \mu F.cm^{-2}$ even though the concentration of inhibitors are approximately same $3.52\times10^{-4}M$, 10^{-4}M and $2.08\times10^{-4}M$.The Fc-1 and Fcfh inhibitors shows high inhibition efficiency (*91.24* %, *91.1* %), then BIM inhibitor (*84.2* %) high IE% consequently due to high surface coverage.

The contradiction of EIS values, attributed to conditions of experiment like: steel specimen kind, temperature and concentration, where they are the main variables in this case.

References:

1. Sanyal, B., *Organic compounds as corrosion inhibitors in different environments—a review.* Progress in Organic Coatings, 1981. **9**(2): p. 165-236.
2. Ergun, Ü., D. Yüzer, and K.C. Emregül, *The inhibitory effect of bis-2, 6-(3, 5-dimethylpyrazolyl) pyridine on the corrosion behaviour of mild steel in HCl solution.* Materials chemistry and physics, 2008. **109**(2-3): p. 492-499.
3. Morad, M. and A. Sarhan, *Application of some ferrocene derivatives in the field of corrosion inhibition.* Corrosion Science, 2008. **50**(3): p. 744-753.
4. El- Awady, A.A., B.A. Abd- El- Nabey, and S.G. Aziz, *Kinetic- thermodynamic and adsorption isotherms analyses for the inhibition of the acid corrosion of steel by cyclic and open- chain amines.* Journal of the Electrochemical Society, 1992. **139**(8): p. 2149.
5. Tawfik, S.M., *Corrosion inhibition efficiency and adsorption behavior of N, N-dimethyl-4-(((1-methyl-2-phenyl-2, 3-dihydro-1H-pyrazol-4-yl) imino) methyl)-N-alkylbenzenaminium bromide surfactant at carbon steel/hydrochloric acid interface.* Journal of Molecular Liquids, 2015. **207**: p. 185-194.
6. McCafferty, E. and N. Hackerman, *Double layer capacitance of iron and corrosion inhibition with polymethylene diamines.* Journal of the Electrochemical Society, 1972. **119**(2): p. 146.
7. Rahim, O., et al., *Evaluation of the inhibitory effectiveness of three ferrocene derivatives for corrosion of steel XC70 by spectroscopy of electrochemical impedance.* Journal of Fundamental and Applied Sciences, 2011. **3**(2): p. 210-223.
8. Radwan, A.B., et al., *Corrosion inhibition of API X120 steel in a highly aggressive medium using stearamidopropyl dimethylamine.* Journal of Molecular Liquids, 2017. **236**: p. 220-231.
9. Khadraoui, A., et al., *Acid extract of Mentha pulegium as a potential inhibitor for corrosion of 2024 aluminum alloy in 1 M HCl solution.* J. Mater. Environ. Sci, 2013. **4**(5): p. 663-670.
10. Orazem, M.E. and B. Tribollet, *Electrochemical impedance spectroscopy.* New Jersey, 2008: p. 383-389.
11. Solomon, M.M., et al., *Exploration of dextran for application as corrosion inhibitor for steel in strong acid environment: effect of molecular weight, modification, and temperature on efficiency.* ACS applied materials & interfaces, 2018. **10**(33): p. 28112-28129.
12. Shukla, S.K. and M. Quraishi, *4-Substituted anilinomethylpropionate: new and efficient corrosion inhibitors for mild steel in hydrochloric acid solution.* Corrosion Science, 2009. **51**(9): p. 1990-1997.

13. Kissi, M., et al., *Establishment of equivalent circuits from electrochemical impedance spectroscopy study of corrosion inhibition of steel by pyrazine in sulphuric acidic solution.* Applied surface science, 2006. **252**(12): p. 4190-4197.
14. Morad, M., *An electrochemical study on the inhibiting action of some organic phosphonium compounds on the corrosion of mild steel in aerated acid solutions.* Corrosion Science, 2000. **42**(8): p. 1307-1326.
15. Gupta, S.R., et al., *Synthesis, structural, electrochemical and corrosion inhibition properties of two new ferrocene Schiff bases derived from hydrazides.* Journal of Organometallic Chemistry, 2014. **767**: p. 136-143.
16. Fatima, S., et al., *Study of new amphiphiles based on ferrocene containing thioureas as efficient corrosion inhibitors: Gravimetric, electrochemical, SEM and DFT studies.* Journal of Industrial and Engineering Chemistry, 2019. **76**: p. 374-387.
17. Nazir, U., et al., *Biferrocenyl Schiff bases as efficient corrosion inhibitors for an aluminium alloy in HCl solution: a combined experimental and theoretical study.* RSC Advances, 2020. **10**(13): p. 7585-7599.
18. Sayed, A.R. and H.M.A. El-Lateef, *Thiocarbohydrazones Based on Adamantane and Ferrocene as Efficient Corrosion Inhibitors for Hydrochloric Acid Pickling of C-Steel.* Coatings, 2020. **10**(11): p. 1068.

Third chapter:

Adsorption isotherms

III.1 Introduction:

The ferrocene compounds study has tremendously increased during the last two decades due to their applications in a variety of areas include additives for heating oil to reduce formation of soot, iron-containing fertilizers [1]. The growing interest of ferrocene derivatives is attributed to their excellent stability towards water and air.

Iron and its alloys are one of the most inspired construction materials for various industrial applications due to their excellent structural and mechanical strength [2]. The poor corrosion resistance of mild steel in acidic solution [3], particularly HCl is used in industrial processes [4], such as acid pickling, acid cleaning, ore production, oil well acidification and acid descaling [3], require a corrosion inhibitor to prevent corrosion of metals during these processes [5], to decrease corrosion phenomenon by adsorption inhibitor on iron surface.

Adsorption of inhibitors on the metal surface involves formation of two types of interaction (physical adsorption and chemical adsorption). Physical adsorption requires the presence of both electrically charged surface of the metal and charged species in the bulk solution. The second one, chemisorptions process involves charge sharing or charge transfer from the inhibitor molecules to the metal surface to form a co-ordinate type bond and takes place in the presence of heteroatom‘s (P, N, S, O, etc.) with lone pairs of electrons and/or aromatic ring in the molecular structure [6-19]. In any case, adsorption is general over the metal surface and the resulting adsorption layer function as a barrier, isolating the metal from the corrosion [20]. The inhibition efficiency has found to be closely related to inhibitor adsorption abilities and molecular properties for different kinds of organic compounds [21-23]. The efficiency of an inhibitor does not only depend on its structure, but also on the characteristics of the environment in which it acts; the nature of the metal, the charge of metal surface [7], and other experimental conditions [24]. In addition, the planarity (π) and lone pair of electrons present on the N atoms are the important structural features that determine the adsorption of these molecules to the metal surface [25].

In this chapter, three ferrocene derivatives namely, Fc-1, Fc-2 and Fc-3 were studied their adsorption isotherm as inhibitors for mild corrosion in 1 M HCl and discussed some of their adsorption properties such as free enthalpy (ΔG^0), which it is considered as inhibition efficiency and their properties were compared with some previous studies.

III.2 Results and discussion

The action of an inhibitor in aggressive acid media is assumed to be due to its adsorption at the metal/solution interface. The adsorption process depends on the electronic characteristics of the inhibitors, the nature of metal surface, temperature, steric effects and the varying degrees of surface-site activity [26]. The adsorption of an organic adsorbate at a metal/solution interface can be regarded as a substitution adsorption process between the organic molecule in the aqueous solution Org_{sol} and the water molecules on the metallic surface H_2O_{ads} [1]:

$$\mathbf{Org_{sol} + (xH_2O)_{ads} \rightleftharpoons Org_{ads} + (xH_2O)_{sol}} \quad (9)$$

X is the size ratio representing the number of water molecules replaced by a molecule of organic adsorbate.

The equations (11, 13 and 15), represent the several adsorption isotherms such as Langmuir, Fig.28, Temkin and Frumkin adsorption isotherms, Fig.29, were used to evaluate the adsorption process and gain mechanistic information about adsorption of Fc-1 (a), Fc-2 (b) and Fc-3 (c) on steel specimen surface.

Langmuir equation:

$$\frac{\theta}{1-\theta} = KC \quad (10)$$

It is linear form:

$$\frac{C}{\theta} = \frac{1}{K} + aC \quad (11)$$

Temkin equation:

$$\theta \exp(g\theta) = KC \quad (12)$$

It is linear form:

$$\mathrm{Log}\left(\frac{\theta}{C}\right) = \mathrm{Log}K - g\theta \quad (13)$$

Frumkin equation:

$$\left(\frac{\theta}{1-\theta}\right)\exp(-g\theta) = KC$$

$$\text{Or } \left(\frac{\theta}{1-\theta}\right)\exp(-2a\theta) = KC \quad (14)$$

It is linear form:

$$\mathrm{Log}\left(\frac{\theta}{(1-\theta)C}\right) = \mathrm{Log}K + g\theta$$

$$\text{Or } \mathrm{Log}\left(\frac{\theta}{(1-\theta)C}\right) = \mathrm{Log}K + 2\alpha\theta \qquad (15)$$

With $g = 2a$

Where C: the inhibitor concentration, α: the parameter of absorbed molecules that interact each other on a metal surface, a: slope, θ: the fraction of surface covered by adsorbed molecules, which was calculated from the Equation (16):

$$\theta = \left(1 - \frac{R_{ct}^{1}}{R_{ct}^{0}}\right) \qquad (16)$$

Where R_{ct}^{0} and R_{ct}^{1} are the charge transfer resistances without inhibition and charge transfer resistance with inhibition respectively, K: equilibrium rate constant of adsorption–desorption phenomenon.

Fig.28, shows Langmuir isotherm of Fc-1 (a), Fc-2 (b) and Fc-3 (c) on XC70 specimen in 1M HCl which the charge transfer resistance (R_{ct}) and double layer capacitance (C_{dl}) values are obtained from the electrochemical impedance spectroscopy study and used to determine the best adsorption isotherm of studied inhibitors, while Table.6, represent Langmuir isotherm to adsorption of Fc-1, Fc-2 and Fc-3 on steel specimen surface.

Table.6. Langmuir isotherm parameters to adsorption process of inhibitors on XC70 specimen in 1M HCl at 25°C.

Compounds	ΔG (kJ/mol)	K (l/mol)	R^2	Slope (a)	Intercept (b)
Fc-1	-35.19	26.55766	0.973	0.98	4E-05
Fc-2	-37.29	61.873	0.983	1.15	2E-05
Fc-3	-34.93	23.862313	0.98	0.94	4E-05

III.2.A **Discussion of Langmuir fitting lines of inhibitors with ideal straight line:**

The Longmuir curve expressed as flowing equation:

$$\frac{C}{\theta} = aC + b \qquad (11, a)$$

Where a is the slope, $b = (\frac{1}{K})$ or it is the inverse of equilibrium constant (K).

When $\theta \to 1$ ($IE = 100\%$) of Eq.11, a, will become: $C = aC$, that mean b is equal to zero (0), so, $K = \frac{1}{b} = \frac{1}{0} = \infty$, that is high negative value, lead to very high negative value of free energy (ΔG°), in

this case the inhibitor molecules fussed on steel surface, and the slope a = 1, the inhibitor molecules adsorbed without interactions, this situation is theoretical never happen in reality.

Fig.28, shows the straight lines of all inhibitors are above ideal line, indicate that the intercept values are not equal to zero (never and ever the intercept to be minus), which means that the molecules adsorbed on steel surface with strong (Chemisorption) or weak (Physisorption), coordination bonds.

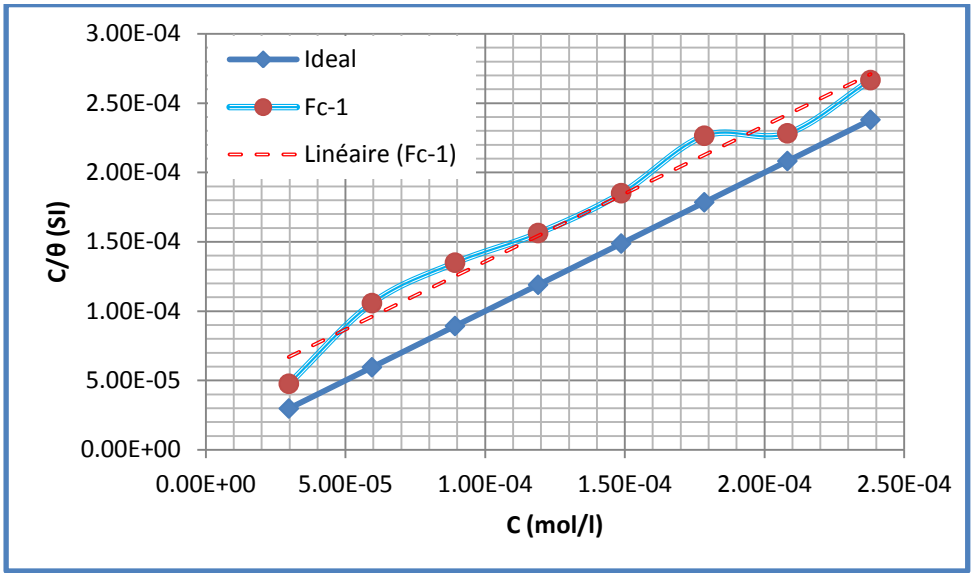

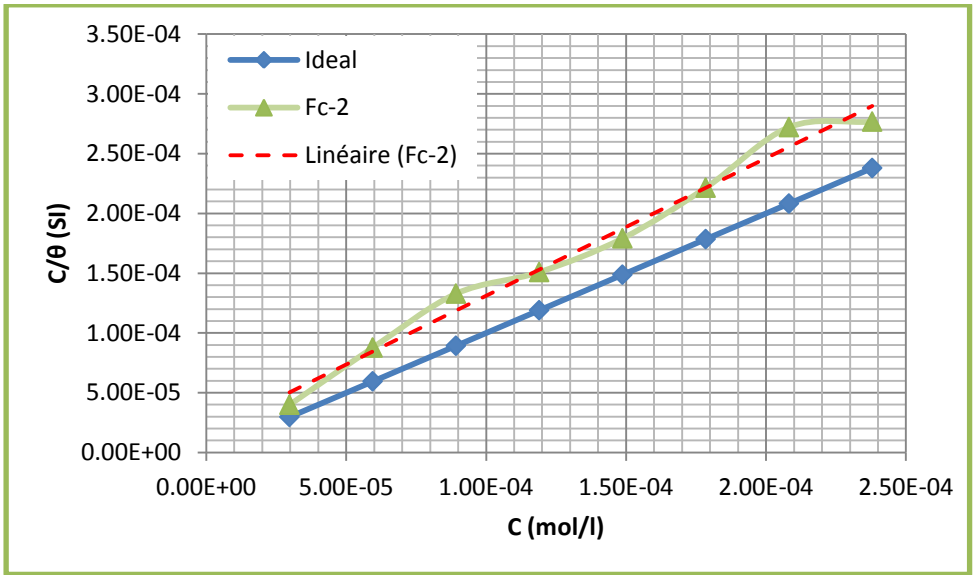

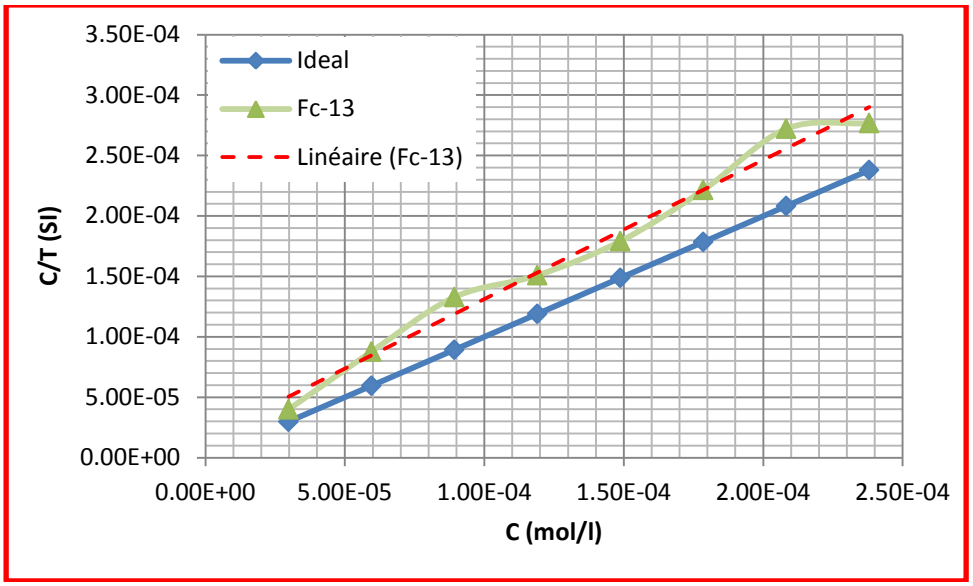

Figuer.28. position of Langmuir fitting lines (Red dashed lines) of inhibitors with ideal straight line (blue), plotted by using Microsoft excel 2007.

Comparing the intercept values of inhibitors, noted that Fc-13's one it's lower than the other ones, that lead to high equilibrium constant (K), consequently, high negative value of Gibb's energy (ΔG^0), that what shown in Table.6.

The slope values of all inhibitors are different of one, which means that the inhibitors adsorbed on steel surface with interactions (attraction or repulsion), between its adjacent molecules, shown in Table.6.

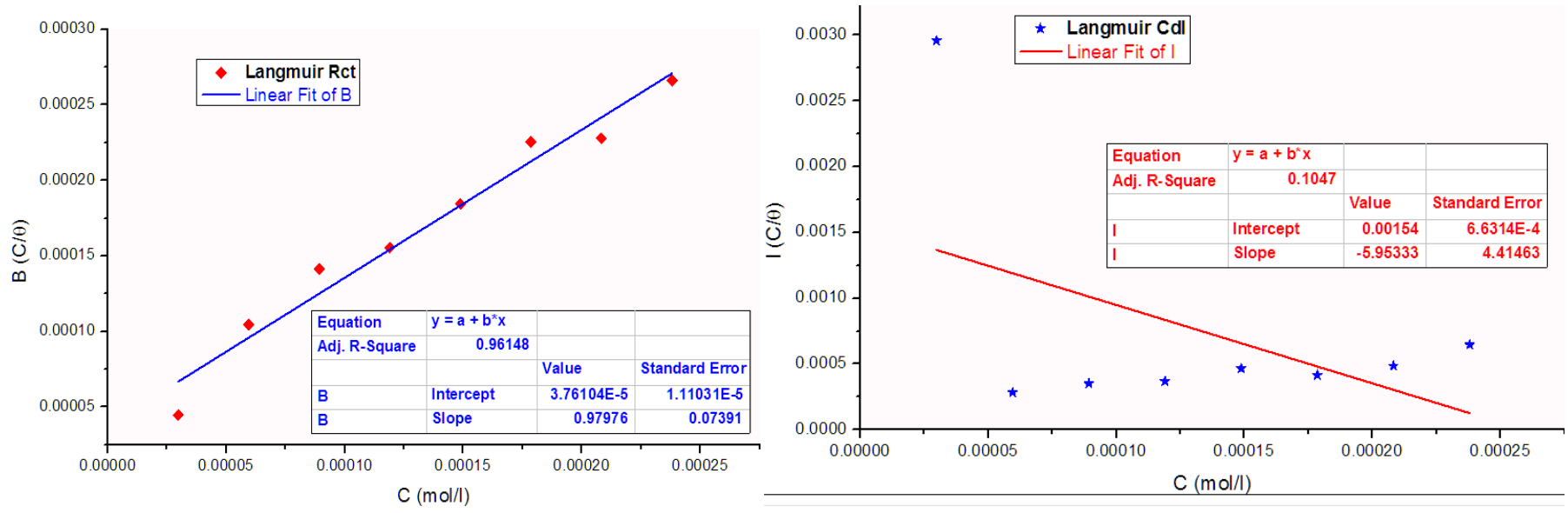

Figure.29.a. Langmuir isotherm of adsorption Fc-1 on XC70 specimen in 1M HCl at 25°C.

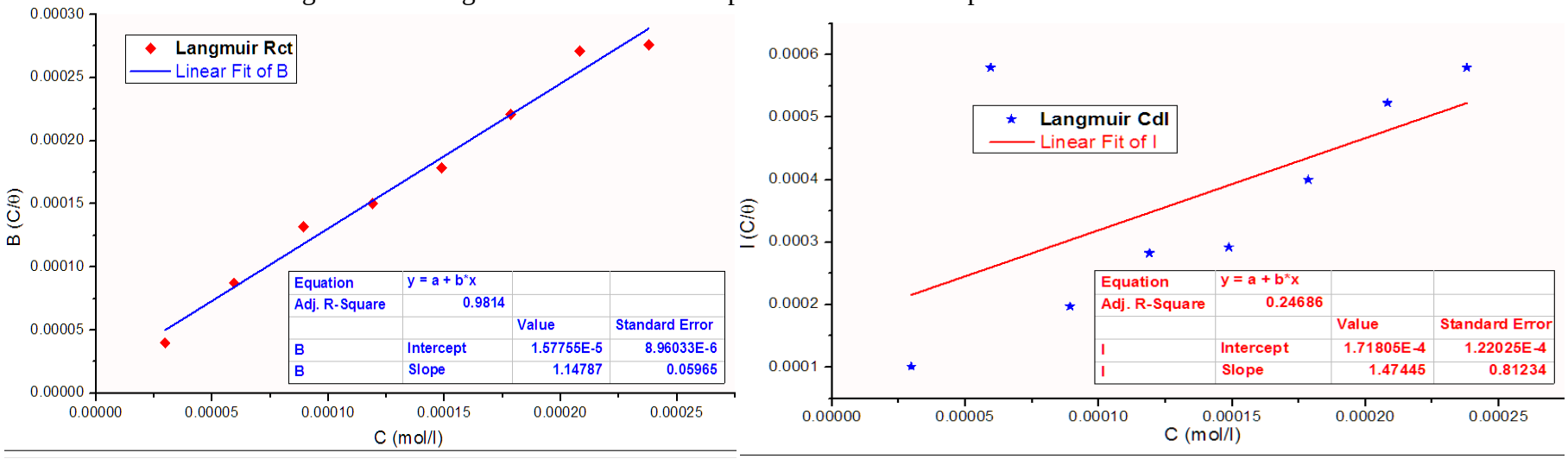

Figure.29.b. Langmuir isotherm of adsorption Fc-2 on XC70 specimen in 1M HCl at 25°C.

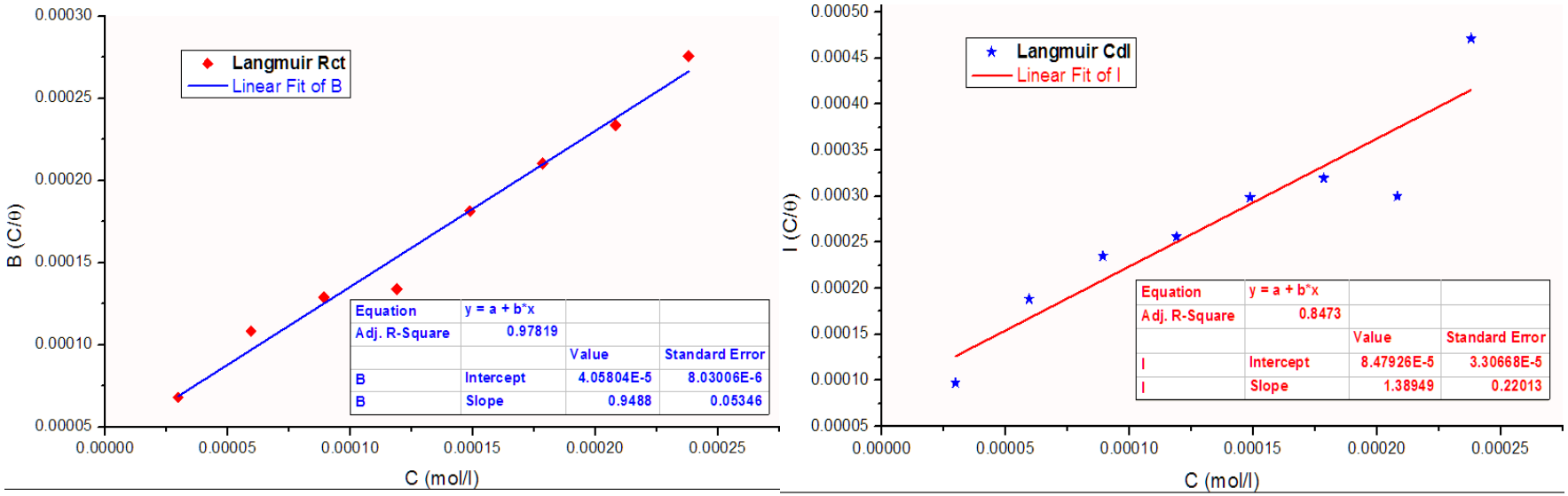

Figure.29.c. Langmuir isotherm of adsorption Fc-3 on XC70 specimen in 1M HCl at 25°C.

III.2.B Regression coefficient discussion (R^2):

A plot of $\frac{C}{\theta}$ versus θ gives regression coefficient 0.9615, 0.9814 and 0.9782 for Fc-1, Fc-2 and Fc-3 respectively, that was for Langmuir isotherm (Fig.29.a, b, c), for Temkin isotherm a plot of Log $\left(\frac{\theta}{C}\right)$ versus θ gives regression coefficient R^2_{Fc-1} = 0.4246, R^2_{Fc-2}= 0.1933 and R^2_{Fc-3} = 0.7211, for Frumkin isotherm a plot of Log $\left(\frac{\theta}{(1-\theta)C}\right)$ versus θ gives regression coefficient R^2_{Fc-1} = -0.02981, R^2_{Fc-2}= -0.1837 and R^2_{Fc-3} = 0.2865, represented in Table.8. The regression coefficient of Langmuir isotherm straight line is equal to unity Table.6, which represent the best fit to adsorption of Fc-1, Fc-2 and Fc-3 on steel specimen surface.

III.2.C Discussion of the slope (α):

The slope less than one (α < 1), indicates the presence of repulsion forces between adsorbed molecules adjacent to each other, the slope equal to 1 (α = 1), denote to adsorption without attraction interaction between the adsorbed molecules, the slope super than one (α > 1), indicates the presence of attraction interaction or repulsion forces between adsorbed molecules, the slope of the straight line. The slope values of Langmuir isotherm (Table.5), for Fc-1, Fc-2 and Fc-3,are 0.98, 1.15 and 0.94 respectively, the slope of Fc-1 and Fc-3 are equal to unity, it could be concluded that they adsorbed on the steel surface following Langmuir isotherm without interaction between the adsorbed molecules. In case of Fc-2 deviation of the slope from unity can be explained in terms of repulsion or attraction of the adsorbed molecules adjacent to each other, a fact which was ignored during the derivation of Langmuir isotherm [1].

III.2.D Discussion of equilibrium constant (K):

The adsorption–desorption equilibrium constant value calculated from the intercept lines on the ($\frac{C}{\theta}$) axis at constant temperature Table.6, it is often used to describe strength of the bond between adsorbent and adsorbate [27], hence, the interactions strength between inhibitors molecules and XC70 steel surface is relatively larger, it indicate that there is strong interaction between adsorbent and adsorbate while smaller value implies a weak interaction. The K values of Fc-1, Fc-2 and Fc-3 inhibitors are found to be $2.656 \times 10^7 M^{-1}$, $6.187 \times 10^7 M^{-1}$ *and* $2.386 \times 10^7 M^{-1}$ respectively, where assumed that the Fc-2 molecules adsorbed on steel surface by strong interactions, whereas weak interactions are formed when Fc-1, Fc-3 molecules are adsorbed on XC70 surface.

The K value is also used to calculate the adsorption standard free energy (ΔG^0) values by following Eq.18:

$$K = \frac{1}{55.5} \exp\left(\frac{-\Delta G^0}{RT}\right) \quad (17)$$

Reciprocating Eq.17:

$$\Delta G^0 = -RT\ln(55.5K) \quad (18)$$

Where the temperature is T in Kelvin, R is universal gas constant $\left(8.314\ \frac{J}{mol.K}\right)$ and 55.5 represents the concentration of water in the solution$\left(\frac{mol}{l}\right)$.

III.2.E **Discussion of Gibb's free energy (ΔG^0):**

The values of ΔG^0 approximately -20 kJ/mol are attributed to electrostatic interaction between charged molecules and charged metal surfaces (physisorption), while values of approximately -40 kJ/mol or more are classified as charge sharing processes or transfer of electrons from the inhibitor molecules to the metal surface to form coordinated bonds (chemisorptions) [28].

As recorded in Table.6, the values of standard Gibb's free energies for Fc-1, Fc-2 and Fc-3 are -39.19 kJ/mol, -37.29 kJ/mol and -34.93 kJ/mol, respectively, calculated using Eq.18. The negative values of ΔG^0 signifies the spontaneity of the adsorption process and stability of the adsorbed inhibitors film on steel surface. The high values of ΔG^0 indicate that adsorption of inhibitors on steel surface in 1 HCl involve both physisorption as well as chemisorptions [3], it is well known that the first step in the inhibition of acid corrosion is the adsorption of inhibitor molecules onto the metal surface. To elucidate the adsorption mechanism, it is necessary to reveal the mode of adsorbed compounds, whether it is physical adsorption (ionic) or chemisorptions (molecular), predominant one of these modes of adsorption over the others depends on several factors, such as the molecular structure of the inhibitor, type of the surface charge [1].

The values of ΔG^0 suggests that adsorption of inhibitors molecules evolve both physical adsorptions which resented by electrostatic interactions and chemical adsorptions which take place via donor-acceptor interaction between lone electronic pairs of hetero-atoms (O, N) and π- electrons of aromatic ring moiety and pentadienyl groups with vacant d-orbitals of the surface iron atoms. In strong acid solutions, ferrocenes undergo extensive protonation on the Fe atom [29], according to the Eq.11. (Fc-2 as an example):

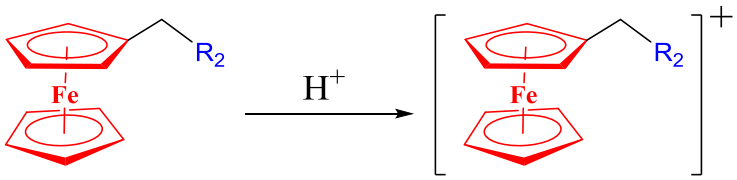

(11)

It is well reported that mild surface becomes positive charged in 1M HCl with respect to the potential of zero charge (PZC) [30], this is what makes chlorine ions (Cl^-) first elements to be excessively

adsorbed on steel surface, as a result of this, the surface of steel becomes excessively negatively charged. At the first stage of adsorption in acid solution, the competition between protonated inhibitors molecules with H^+ for electrons, might be due to absorb them on the steel surface by electrostatic interactions which is responsible for the physical adsorption of positively charged inhibitors molecules. However, after H_2 released as a gas, the inhibitors molecules returns to their neutral form and bonding on steel surface through interaction by free electronic pairs of hetero-atoms (O, N) and π- electrons of benzene and pentadienyl group with empty d-orbitals of Fe atoms (donor-acceptor), this cause an excessive build-up of negative charge on steel surface, in order to reduce the negative charges stacked on steel surface the electrons may be transferred from the d-orbital of iron to anti-bonding (π^*) molecular orbitals of the inhibitor molecules, this can gives it more surface to adsorption. Therefore, the inhibitors may absorb on steel surface by following ways: (a) electrostatic interactions between positively charge inhibitors and adsorbed chlorine ions (Cl^-) (physisorption), (b) interactions between heteroatom's unshared lone electronic pairs and π- electrons of aromatic rings and pentadienyl groups with empty d-orbital of surface Fe atoms (chemisorptions), (c) interactions between d-orbital of surface iron atoms and vacant anti-bonding (π^*) molecular orbital of the inhibitor molecule (retro donation).

According to the ΔG^0 values, the efficiency order of inhibitors is as follows: **Fc-2** > **Fc-3** > **Fc-1**. The order of inhibition efficiency can be explained on basis the intermolecular repulsion of Fc-12 molecule which it is with lone pair electron of the nitrogen (N) atom and lone electronic pairs of oxygen atoms of nitro group (NO_2) in the ortho position, not to mention their resonance effect which they are very close to each other which reduce the formation of stable complex through a simple coordination bond with the XC70 surface through the lone electronic pairs of the nitrogen and oxygen atoms, this causes the adsorption of the protection layer to be weakened. Consequently, the inhibition of iron corrosion reduced. However, the presence of NO_2 group in the metha position of Fc-2 molecule reduces the intermolecular repulsion, gives the compound more stability and enhances the interaction strength of protective layer to impart the inhibition of XC70 surface. Finally, Fc-3 comes at the middle of all compounds in its percentage inhibition efficiency value, owing to the presence of NO_2 group in the para position to Fc-1.

Table.7. List of various synthesizes inhibitors that are being studied their adsorption isotherm on various metals surface in HCl and H_2SO_4 medium.

Num	Inhibitor(s)	Medium(s)	Methods	Results					Reference
				Adsorption Isotherm Study					
					ΔG (kJ/mol)	K (1/M)	Slope	Adsorption isotherm	
1	Diacetyl Fc, Diformyl Fc & BIM Fc	0.5 M H_2SO_4 and 1 M HCl	PDP	Diformyl Fc	-9.78	8.85E-01	≈ 1	**Langmuir**	[1]
				Diacetyl Fc	/	/	> 1		
				BIM Fc	-54.50	4.67E+07	-3.6	**Frumkin**	
				➢ **At 30°C in 0.5 M H_2SO_4**					
2	Fc-22, Fc-23 & Fc-24	0.5 M H_2SO_4	PDP	Fc-22	-38.41	9.75E+07	1.278	**Langmuir**	[31]
				Fc-23	-34.70	2.18E+07	0.986		
				Fc-24	-35.58	3.12E+07	1.799		
				➢ **At 25°C**					
3	M-11, M-13, M-17	1 M HCl	WLS	M-11	-39.52	2.81E-04	1.01	**Langmuir**	[32]
				M-13	-40.51	4.08E-04	0.98		
				M-17	-41.94	6.85E-04	0.98		
				➢ **1mM at 60°C**					

4	Fe-Th	1 M HCl	EIS	Fe-Th	-41.03	7.80E+04	≈ 1	**Langmuir**	[33]
				➢ **200ppm at 50°C**					
5	Fc-1, Fc-2 and Fc-3	1 M HCl	EIS	Fc-1	-39.19	2.66E+07	0.980	**Langmuir**	[34]
				Fc-2	-37.29	6.19E+07	1.150		
				Fc-3	-34.93	2.39E+07	-1.590		
				➢ **At 25°C**					

EIS – Electrochemical impedance spectroscopy, WLS – Weight loss study, PDP – Potentio-dynamic polarization

III.3 Conclusion:

The inhibition efficiency and the method performance based on ferrocene moiety, containing NO_2 group in different positions on aromatic ring have been compared with previously reported ferrocene based inhibitors as shown in Table.7.

The comparing adsorption isotherm of Fc-2 inhibitor with those of Oumelkheir et al. [31], who studied the effect of 2-(ferrocenyl methyl) aminobenzonitrile (Fc-22) and other ferrocene derivatives on mild steel corrosion in 0.5M H_2SO_4 solution. They found that Fc-22 is strongly adsorbed (chemisorption) on steel surface with free enthalpy $\Delta G^0 = -38.41$ *kJ/mol*, it is less then Fc-2's free enthalpy, slight difference in energy between them, that because of Fc-22 make bonds only through N atom that contained $C \equiv N$ group and Fc-2 containing NO_2 group which make more coordination bonds through lone pairs of electrons of N and O atoms.

While when Fc-2 compared with those of M.S. Morad, A.A.O. Sarhan [1], who studied the effect of some ferrocene derivatives (Diacetyl Fc, Diformyl Fc, BIM Fc) on mild steel corrosion in HCl and H_2SO_4 solution at temperature 30°C. They found that the compounds have low inhibition efficiency in 1 M HCl, while BIM Fc shows high efficiency in 0.1 M H_2SO_4 that is according to free enthalpy equal to -54.5*kJ/mol* at temperature 30°C.

The comparing adsorption isotherm when Fc-1 compared with those of S. Fatima et al. [32], who studied the effect of (octadecanoyl)-3-(4-ferrocenyl-2-methylbenzyl) thiourea (M-17) and some ferrocene derivatives (M-11, M-13) on mild steel corrosion in 1M HCl solution at same temperature and different concentration ($10^{-3}M$).

They mention that M-17 is strongly adsorbed (chemisorption) on steel surface with ΔG^0 = *-36.92 kJ/mol*. Indicate that, M-17 is much weak as an inhibitor for the corrosion of carbon steel in 1M HCl solution than Fc-1. This could be refer to long chain of hydrocarbon ($C_{17}H_{35}$) that attach to the carbonyl group of N-carbamothioylacetamide moiety, hence the observed reduction of the inhibition efficiency of M-17.

Unlike, the effect of 2-(ferrocenyl-1-ylidene) hydrazinecarbothiohydrazide (Fe-Th) on mild steel corrosion in 1M HCl solution at temperature 50°C and concentration 200 *ppm*, that were studied by Abdelwahed R et al. [33]. They found that Fe-Th is strongly adsorbed (chemisorption) ($\Delta G^0 = -41.03$ *kJ/mol*). Obviously, the Fe-Th molecule is much better as an inhibitor for the corrosion of mild steel in HCl solution than Fc-1. This could be attributed to the presence of sulfur (S) atom and additional nitrogen (N) of hydrazinecarbothiohydrazide moiety and their high electron releasing tendency which ensure high electron densities at the adsorption sites of Fe-Th and thereby increasing the adsorption

process. Increasing in the adsorption process could be enhanced by increase the concentration or raising the temperature, consequently the inhibition efficiency increased.

References:

1. Morad, M. and A. Sarhan, *Application of some ferrocene derivatives in the field of corrosion inhibition.* Corrosion Science, 2008. **50**(3): p. 744-753.
2. Yıldız, R., *An electrochemical and theoretical evaluation of 4, 6-diamino-2-pyrimidinethiol as a corrosion inhibitor for mild steel in HCl solutions.* Corrosion Science, 2015. **90**: p. 544-553.
3. Verma, C., M. Quraishi, and A. Singh, *A thermodynamical, electrochemical, theoretical and surface investigation of diheteroaryl thioethers as effective corrosion inhibitors for mild steel in 1 M HCl.* Journal of the Taiwan Institute of Chemical Engineers, 2016. **58**: p. 127-140.
4. Ji, G., et al., *Inhibitive effect of Argemone mexicana plant extract on acid corrosion of mild steel.* Industrial & Engineering Chemistry Research, 2011. **50**(21): p. 11954-11959.
5. Allaoui, M., O. Rahim, and L. Sekhri, *Electrochemical study on corrosion inhibition of iron in acidic medium by Moringa Oleifera extract.* Oriental Journal of Chemistry, 2017. **33**(2): p. 637-646.
6. Emregül, K.C., R. Kurtaran, and O. Atakol, *An investigation of chloride-substituted Schiff bases as corrosion inhibitors for steel.* Corrosion Science, 2003. **45**(12): p. 2803-2817.
7. Obot, I., N. Obi-Egbedi, and S. Umoren, *Antifungal drugs as corrosion inhibitors for aluminium in 0.1 M HCl.* Corrosion Science, 2009. **51**(8): p. 1868-1875.
8. Quartarone, G., L. Bonaldo, and C. Tortato, *Inhibitive action of indole-5-carboxylic acid towards corrosion of mild steel in deaerated 0.5 M sulfuric acid solutions.* Applied surface science, 2006. **252**(23): p. 8251-8257.
9. Bentiss, F., et al., *Effect of iodide ions on corrosion inhibition of mild steel by 3, 5-bis (4-methylthiophenyl)-4H-1, 2, 4-triazole in sulfuric acid solution.* Journal of Applied Electrochemistry, 2002. **32**(6): p. 671-678.
10. Bentiss, F., et al., *Enhanced corrosion resistance of mild steel in molar hydrochloric acid solution by 1, 4-bis (2-pyridyl)-5H-pyridazino [4, 5-b] indole: Electrochemical, theoretical and XPS studies.* Applied Surface Science, 2006. **252**(8): p. 2684-2691.
11. Bentiss, F., M. Lebrini, and M. Lagrenée, *Thermodynamic characterization of metal dissolution and inhibitor adsorption processes in mild steel/2, 5-bis (n-thienyl)-1, 3, 4-thiadiazoles/hydrochloric acid system.* Corrosion Science, 2005. **47**(12): p. 2915-2931.
12. Bentiss, F., et al., *On the relationship between corrosion inhibiting effect and molecular structure of 2, 5-bis (n-pyridyl)-1, 3, 4-thiadiazole derivatives in acidic media: Ac impedance and DFT studies.* Corrosion Science, 2011. **53**(1): p. 487-495.
13. Chetouani, A., et al., *New synthesised pyridazine derivatives as effective inhibitors for the corrosion of pure iron in HCl medium.* Progress in Organic Coatings, 2002. **45**(4): p. 373-378.

14. Khaled, K., K. Babić-Samardžija, and N. Hackerman, *Theoretical study of the structural effects of polymethylene amines on corrosion inhibition of iron in acid solutions.* Electrochimica Acta, 2005. **50**(12): p. 2515-2520.
15. Wang, H.-L., R.-B. Liu, and J. Xin, *Inhibiting effects of some mercapto-triazole derivatives on the corrosion of mild steel in 1.0 M HCl medium.* Corrosion Science, 2004. **46**(10): p. 2455-2466.
16. Bouklah, M., et al., *Thiophene derivatives as effective inhibitors for the corrosion of steel in 0.5 M H2SO4.* Progress in organic coatings, 2004. **49**(3): p. 225-228.
17. Lebrini, M., et al., *Inhibitive properties, adsorption and a theoretical study of 3, 5-bis (n-pyridyl)-4-amino-1, 2, 4-triazoles as corrosion inhibitors for mild steel in perchloric acid.* Corrosion science, 2008. **50**(2): p. 473-479.
18. Popova, A., et al., *Adsorption and inhibitive properties of benzimidazole derivatives in acid mild steel corrosion.* Corrosion science, 2004. **46**(6): p. 1333-1350.
19. Quraishi, M. and D. Jamal, *Inhibition of mild steel corrosion in the presence of fatty acid triazoles.* Journal of Applied Electrochemistry, 2002. **32**(4): p. 425-430.
20. Ebenso, E., *Effect of halide ions on the corrosion inhibition of mild steel in H2SO4 using methyl red: Part 1.* Bulletin of Electrochemistry, 2003. **19**(5): p. 209-216.
21. Bereket, G., C. Öğretir, and A. Yurt, *Quantum mechanical calculations on some 4-methyl-5-substituted imidazole derivatives as acidic corrosion inhibitor for zinc.* Journal of Molecular Structure: THEOCHEM, 2001. **571**(1-3): p. 139-145.
22. Khalil, N., *Quantum chemical approach of corrosion inhibition.* Electrochimica Acta, 2003. **48**(18): p. 2635-2640.
23. Costa, J. and J. Lluch, *The use of quantum mechanics calculations for the study of corrosion inhibitors.* Corrosion science, 1984. **24**(11-12): p. 929-933.
24. Madkour, L. and S. Elroby, *Correlation between corrosion inhibitive effect and quantum molecular structure of Schiff bases for iron in acidic and alkaline media.* Nature, 2014. **2**: p. 680-704.
25. Prabhu, R., et al., *Quinol-2-thione compounds as corrosion inhibitors for mild steel in acid solution.* Materials Chemistry and Physics, 2008. **108**(2-3): p. 283-289.
26. El- Awady, A.A., B.A. Abd- El- Nabey, and S.G. Aziz, *Kinetic- thermodynamic and adsorption isotherms analyses for the inhibition of the acid corrosion of steel by cyclic and open- chain amines.* Journal of the Electrochemical Society, 1992. **139**(8): p. 2149.

27. Kaczerewska, O., et al., *Effectiveness of O-bridged cationic gemini surfactants as corrosion inhibitors for stainless steel in 3 M HCl: Experimental and theoretical studies.* Journal of Molecular Liquids, 2018. **249**: p. 1113-1124.
28. Radwan, A.B., et al., *Corrosion inhibition of API X120 steel in a highly aggressive medium using stearamidopropyl dimethylamine.* Journal of Molecular Liquids, 2017. **236**: p. 220-231.
29. Rosenblum, M., *Chemistry of the iron group metallocenes: ferrocene, ruthenocene, osmocene*. 1965: Interscience Publishers.
30. Deng, S., X. Li, and H. Fu, *Acid violet 6B as a novel corrosion inhibitor for cold rolled steel in hydrochloric acid solution.* Corrosion Science, 2011. **53**(2): p. 760-768.
31. Rahim, O., K. Chaouche, and T. Lanez, *Pouvoir Inhibiteur de la Corosion Aqueuse par Quelques Amines Ferroceniques.* Annals of Science and Technology, 2013. **5**(1): p. 9-9.
32. Fatima, S., et al., *Study of new amphiphiles based on ferrocene containing thioureas as efficient corrosion inhibitors: Gravimetric, electrochemical, SEM and DFT studies.* Journal of Industrial and Engineering Chemistry, 2019. **76**: p. 374-387.
33. Sayed, A.R. and H.M.A. El-Lateef, *Thiocarbohydrazones Based on Adamantane and Ferrocene as Efficient Corrosion Inhibitors for Hydrochloric Acid Pickling of C-Steel.* Coatings, 2020. **10**(11): p. 1068.
34. Rahim, O., et al., *Evaluation of the inhibitory effectiveness of three ferrocene derivatives for corrosion of steel XC70 by spectroscopy of electrochemical impedance.* Journal of Fundamental and Applied Sciences, 2011. **3**(2): p. 210-223.

Fourth chapter:

Quantum Chemical Calculations

IV.1 Method and materials:

The quantum chemical calculation is wonderful technique that used to calculate and predicte the propreties for unknown molecules.
HyperChem is used on geometry optimization to calculate propreties QSAR of titled compounds, with tow force fields: Amber99, MM+ and one method: ZINDO1 (using Algorithm: Polak-Ribiere and 0.01kcal/$A^{\circ 2}$.mol as RMS), while the quantum chemical calculations on the optimized structures were performed using Gaussian software package using density functional theory (DFT) presented by B3LYP hybrid function with 6-31G(d,p) and LanL2DZ basis set.
The comparation between Gaussian and HyperChem methods with experimental results, allow us to obtain the best theoretical method to applied for this kind of compounds (organo-iron).
The Fc-1 properties that mesured by X-Ray [1], are used as a referance to compare it with all methodes.
Avogadro program version 1.1.1 was used to draw the molecules.
Chem3D 16.0 PerkinElmer was used to obtain the bond lengths and bond angles measurements.

IV.1.A **Work steps:**

- With HyperChem:
  - Open Avogadro program and draw the molecule.
  - Save it as MDL SDfile (*.mol) route.
  - Open .mol file using HperChem program.
  - Go to Setup to choice the method.
  - Click on compute and choice Geometry Optimization calculation. After the calculations are complete save it (Ctrl+S) as MOL2 (*.ml2) route, and open it using Chem3D.
  - From Structure click on Measurements and choice Generate All Bond Lengths and Angles.
- With Gaussian:
  - Open Avogadro program and draw the molecule.
  - Go to Extensions and click on Gaussian.
  - Choice the Calculation and Theory and Basis.
  - Click on Generate and save it (*.com).
  - Go to Gaussian and open the file.
  - Click on star botton (Up-Right) and save it as (*.out) route.
    After the calculations are completes
  - Using Avogadro program open .out file and save it as MDL SDfile (*.mol) route.
  - open .ml2 file using Chem3D to Generate All Bond Lengths and Bond Angles.
    Or open .out file using Notepad to extract the measurements.

IV.1.B **Programs that used:**

→ Gaussian 09 Revision D.01 Release Notes 29 April 2013.
→ HyperChem 8.08.
→ Avogadro version 1.1.1.
→ Chem3D 16.0 PerkinElmer.

IV.2 Results and discussion

IV.2.A **Comparation between methods:**

Table.8. the stability energy of Fc-1 calculated using HyperChem and Gaussian methods.

	HyperChem			Gaussian	
	ZINDO/1	**Amber99**	**MM+**	**6-31G(d,p)**	**LanL2DZ**
Energy (kcal/mol)	-12392.41	1581.517	699.366	-2180.95 H.a.u	-1040.586 H.a.u
Gradient	1.691	0.084	0.090	3×10^{-6}	6×10^{-6}

The stability of compounds revealed form their energies, which high energy value indicate that easy to react or low stability, due to repulsion forces between the atoms (intramlecular), while low energy indicate to high stability.

As shown in Table.8, the energy value that obtined by ZINDO1 method (HyperChem), shows low energy value (-12392.41 kcal/mol), while Amber99 and MM+ fields have high energy values (1581.517 kcal/mol, 699.366 kcal/mol, in order), it means that the ZINDO1 field it is better than Amber99 and MM+ fields.

Whereas, the 6-31G(d,p) basis set that used by Gaussian program, shows low energy value (-2180.94982 a.u) compare to LanL2DZ basis set (-1040.586 a.u), which 6-31G(d,p) it is better than LanL2DZ to use as basis set to these kind of compounds.

The comparation of energies that obtained by 6-31G(d,p) basis set and ZINDO1, found that the 6-31G(d,p) has low energy value than ZINDO1, which it is better method to applied to these kind of compounds.

Hartree atomic unit (H.a.u) was converted to kcal/mol by using following laws:

1 Hartree = 4.3597×10^{-18} J
1 Hartree = 27.21139 ev

-2180.95 Hartree = -1368546.125 kcal/mol
-1040.59 Hartree = -652970.225 kcal/mol

Table.9. Bond lengths and angles of Fc-1 calculated using HyperChem and Gaussian methods.

Bonds		X-Ray	HyperChem ZINDO/1	HyperChem Amber99	HyperChem MM+	Gaussian 6-31G(d,p)	Gaussian LanL2DZ
Lengths (A°)	**H-C**	0.935	1.096	1.083	1.076	1.096	**1.027**
	C-C	1.439	**1.425**	1.499	1.472	1.424	1.419
	C-Fe	2.067	2.258	1.946	2.136	**2.046**	2.118
	C-N	1.432	1.411	**1.434**	**1.434**	1.422	1.427
	N-O	1.249	1.233	1.2565	1.258	**1.241**	1.294
	N-H	0.83	**0.999**	**0.999**	**0.999**	1.014	1.019
Angles (°)	**H-C-Fe**	126.609	**127.145**	115.459	100.779	-	-
	C-C-H	122.907	**123.273**	121.382	120.435	116.391	120.012
	C-C-C	114.067	**114.069**	112.98	113.707	114.013	114.014
	C-C-Fe	72.178	**71.485**	66.491	69.411	89.211	70.314
	C-Fe-C	99.362	99.811	91.899	**99.094**	-	140.487

	C-C-N	119.276	118.373	118.245	118.79	**119.381**	111.232
	H-N-C	117.15	116.437	113.235	117.672	59.349	**116.708**
	H-C-N	108.9	**109.145**	109.620	108.548	110.004	108.495
	O-N-C	119.11	120.209	120.895	120.793	**119.024**	119.458
	O-N-O	121.78	117.733	117.733	117.733	**121.953**	121.084
	C-N-C	125.3	**124.228**	**124.228**	**124.228**	126.443	126.387
	H-C-H	107.7	**107.508**	**107.508**	**107.508**	**107.508**	106.022

The numbers that close to X-Ray's mesurments are colored by gras red color, shown in Table.9, which represents the Average of bond lengths and bond angles.

Table.10. QSAR properties of Fc-1 calculated using HyperChem and Gaussian methods.

	ZINDO/1	Amber99	MM+	6-31G(d,p)	LanL2DZ
Hydration Energy	-3.52	-3.91	-4.44	-16.41	-6.8
Log P	-4.77	-4.77	-4.77	-1.6	-2.92
Refractivity	76.9	76.9	76.9	77.06	82.16
Polarizability	29.18	29.18	29.18	31.8	31.51
Mass	336.17	336.17	336.17	336.17	336.17
Surface Area (Approx)	306.76	297.26	319.3	32.74	371.84
Surface Area (Grid)	501.01	461.01	474.09	502.09	495
Volume	844.05	795.27	833.15	847.74	843.67

The solubility of compounds can be predicted by Partition coefficiant (Log P), perperesent the concentratin value between [n-octanol]/[water], which octanol indicate the organic solvants or apolar solvants, when the water indicate polar solvants. The ability of compound to dissolve in organic solvants related to high value of log P, and the low value indicate to the ability of compound to disolve in organic solvants.

Table.10, show that Fc-1 is very soluble in water for all HyerChem methods with a same value (-4.77), and decrease with Gaussian methods from -2.92 for LanL2DZ to -1.6 for 6-31G(d,p) .

IV.2.B **Comparation between molecules:**

Table.11. the energy of inhibitors calculated using MM+ force field.

	HyperChem		
	Fc-12	Fc-13	Fc-14
Energy(kcal/mol)	699.366	697.522	699.539
Gradient	0.0903	0.0986	0.0998

The Fc-1, Fc-2 and Fc-3 inhibitors energy (Table.11) are found by using MM+ force field to be 699.366 kcal/mol, 697.522 kcal/mol and 699.539 kcal/mol, respetivaley, exhibit that Fc-2 is more stable.

Table.12. Bond lengths and bond angles of inhibitors calculated using MM+ force field.

Bonds		Fc-12	Fc-13	Fc-14
Lengths (A°)	**H-C**	1.078	1.078	1.078
	C-C	1.472	1.472	1.472
	C-Fe	2.136	2.136	2.136
	C-N	1.433	1.434	1.434
	N-O	1.258	1.257	1.258
	N-H	0.999	0.999	0.999
Angles (°)	**H-C-Fe**	100.779	100.788	100.803
	C-C-H	120.435	120.422	120.200
	C-C-C	113.707	113.718	113.723
	C-C-Fe	69.411	69.412	69.411
	C-Fe-C	99.094	99.122	99.106
	C-C-N	118.79	118.806	118.937
	H-N-C	117.672	117.441	117.388
	H-C-N	108.548	109.190	109.194
	O-N-C	120.793	121.159	121.147
	O-N-O	117.733	117.681	117.705
	C-N-C	124.228	124.503	124.391
	H-C-H	107.508	107.293	107.356

Table.12, show the H-C, C-C, H-N and C-Fe bonds length are same for all inhibitors, while N-O bond of Fc-2 has a small length then Fc-1 and Fc-3.

Table.13. QSAR properties of inhibitors calculated using MM+ force field.

	Fc-12	Fc-13	Fc-14
Hydratation Energy	-4.44	-6.3	-6.43
Log P	-4.77	-4.77	-4.77
Refractivity	76.9	76.9	76.9
Polarizability	29.18	29.18	29.18
Mass	336.17	336.17	336.17
Surface Area (Approx)	319.3	356.9	357.03
Surface Area (Grid)	474.09	494.74	492.59
Volume	833.15	848.53	847.38

IV.3 Conclusion:

The comparation between methods and X-Ray measurements, occur that the ZINDO/1 method is the best method to predict the organo-iron compounds measurements, whereas 6-31G (d,p) basis set shows lowest energy value with lowest gradient, and records highest value of Log P (-1.6) than other methods, which spouse to poor solubility of inhibitors in solutions, noted in chapter Ⅱ.

The comparation between stabilization energy of inhibitors using MM+ reveals that the Fc-2 inhibitor is more stable, while Log P value of inhibitors are negative (-4.77), indicate that the compound is too hydrophilic it has good aqueous-solubility.

General conclusion:

According to what has been discussed in this theoretical comparative study, conclude that the Fc-1 has tendency to form an isolate layer on the metal surface, related to its high R_{ct} ($533.122\ ohm.cm^2$), also, shows high inhibition efficiency ($91.24\ \%$), while Fc-3 record low double layer capacitance indicated ($84.674\ \mu F/cm^2$) with concentration $70ppm$ at $25°C$.

Fcuc inhibitor has high charge transfer resistance ($3198\ ohm.cm^2$), also, exhibit high inhibition efficiency ($97\ \%$) with concentration $100ppm$ at $25°C$, that lead to Fcuc molecules has more trend to form an adsorbed protective layer on the metal surface, compare to Fc-1 inhibitor, whereas, low value of double layer capacitance indicated for Fc-Th inhibitor ($39.6\ \mu F.cm^{-2}$) with concentration $200ppm$ at $25°C$, compare to Fc-3 inhibitor.

Conclude that the Fc-2 is the best as an inhibitor in 1M HCl solution, which its form strong interactions with XC70 steel surface, that is according to its high adsorption–desorption equilibrium constant ($6.187 \times 10^7 M^{-1}$). The high negative value of standard free enthalpy (-39.19 kJ/mol) at 25°C, reveal the fact that it's strongly adsorbed (chemisorption) on XC70 steel surface with spontaneously process.

According to comparation part, Fc-2 show high adsorption–desorption equilibrium constant ($6.187 \times 10^7 M^{-1}$), at 25°C, while, the high negative value of free enthalpy (-41.03 kJ/mol), related to Fe-Th inhibitor at 50°C in 1M HCl solution, whereas at temperature 30°C and in 0.1 M H_2SO_4 free enthalpy of BIM Fc -54.5kJ/mol.

The comparation between methods and X-Ray measurements, occur that the ZINDO/1 method is the best method that used to predict an organo-iron compounds measurements, whereas 6-31G (d,p) basis set shows lowest energy value (more stabilization) with lowest gradient (more accurate).

The comparation of stabilization energy between inhibitors using MM+, reveals that the Fc-2 inhibitor is more stable than other.

Recommendations for Future research:

For future research, a comparison study between various Gaussian methods should be made, not just with X-Ray measurements also with other experimental technique such as X-Ray fluorescence (XRF), X-Ray diffraction (XRD) and proton-induced x-ray emission (PIXE) to obtain more accurate method, especially for this kind of compounds, and discussion a mathematical equation that calculate Log P.

References:

1. Rahim, O., et al., *N-Ferrocenylmethyl-2-nitroaniline*. Acta Crystallographica Section E: Structure Reports Online, 2012. **68**(10): p. m1318-m1318.

http://journals.iucr.org/e/services/newformat.html

Appendices

Electrochemical impedance spectroscopy (EIS) features of the XC70 steel in 1M HCl.

			R_{ct} (ohm.cm^2)	IE%	Θ	f_{Max} (Hz)	C_{dl}(µF.cm^{-2})	IE%	θ
HCl			**45.9870**	**-**	**-**	**31.646**	**276.5490**	**-**	**-**
Blank			**46.6930**	**-**	**-**	**31.646**	**278.8030**	**-**	**-**
Fc-1	10	2.97E-05	137.931	66.148	0.661	16.250	273.766	1.807	0.018
	20	5.95E-05	106.737	56.254	0.563	20.000	218.508	21.626	0.216
	30	8.92E-05	124.527	62.504	0.625	16.250	206.361	25.983	0.260
	40	1.19E-04	195.623	76.131	0.761	12.500	187.176	32.864	0.329
	50	1.49E-04	238.004	80.381	0.804	10.218	188.241	32.483	0.325
	60	1.78E-04	220.448	78.819	0.788	12.500	157.248	43.599	0.446
	70	2.08E-04	533.122	91.242	0.912	5.000	157.907	43.363	0.434
	80	2.38E-04	434.800	89.261	0.893	6.468	174.686	37.344	0.373
Fc-2	10	2.97E-05	183.117	74.501	0.745	12.500	194.918	30.088	0.301
	20	5.95E-05	144.942	67.785	0.678	12.500	248.148	10.995	0.110
	30	8.92E-05	142.143	67.151	0.672	20.000	151.407	45.694	0.457
	40	1.19E-04	220.520	78.826	0.788	12.500	159.998	42.612	0.426
	50	1.49E-04	275.195	83.033	0.830	12.500	135.650	51.346	0.513
	60	1.78E-04	240.385	80.576	0.806	12.500	153.103	45.086	0.451
	70	2.08E-04	198.701	76.501	0.765	12.500	166.370	40.327	0.403
	80	2.38E-04	332.987	85.978	0.860	7.937	162.954	41.552	0.416
Fc-3	10	2.97E-05	81.643	42.808	0.428	31.646	192.043	31.119	0.311
	20	5.95E-05	101.886	54.171	0.542	25.823	189.223	32.130	0.321
	30	8.92E-05	149.143	68.692	0.687	20.000	171.526	38.478	0.385
	40	1.19E-04	412.012	88.667	0.887	7.937	148.023	46.908	0.469
	50	1.49E-04	254.724	81.669	0.817	12.500	138.848	50.199	0.502
	60	1.78E-04	303.400	84.610	0.846	12.500	122.061	56.220	0.562
	70	2.08E-04	424.643	89.004	0.890	10.218	84.674	69.630	0.696
	80	2.38E-04	335.318	86.075	0.861	10.218	136.890	50.900	0.509
	C(ppm)	C(mol/l)							

The impedance magnitude slope (*S*) and phase angle (Φ) obtained for XC70 steel in 1M HCl.

	C (M)	Slope (S)	R^2	Phase angle (Φ)
Fc-1	2.97E-05	-0.6961	0.9996	-59.12
	5.95E-05	-0.6843	0.9995	-57.49
	8.92E-05	-0.7036	0.9996	-59.86
	1.19E-04	-0.7262	0.9997	-61.69
	1.49E-04	-0.7301	0.9998	-62.4
	1.78E-04	-0.735	0.9998	-62.33
	2.08E-04	-0.7821	0.9999	-67.17
	2.38E-04	-0.7624	0.9998	-65.22
Fc-2	2.97E-05	-0.7169	0.9997	-60.89
	5.95E-05	-0.7028	0.9997	-59.76
	8.92E-05	-0.7175	0.9997	-60.59
	1.19E-04	-0.746	0.9998	-63.12
	1.49E-04	-0.7604	0.9997	-64.61
	1.78E-04	-0.7456	0.9998	-63.2
	2.08E-04	-0.7275	0.9998	-61.95
	2.38E-04	-0.7623	0.9999	-64.96
Fc-3	2.97E-05	-0.6602	0.999	-55.37
	5.95E-05	-0.6968	0.9994	-58.93
	8.92E-05	-0.7056	0.9997	-59.88
	1.19E-04	-0.7591	0.9998	-64.92
	1.49E-04	-0.7362	0.9999	-62.9
	1.78E-04	-0.7509	0.9998	-63.99
	2.08E-04	-0.7771	0.9998	-66.66
	2.38E-04	-0.753	0.9998	-64.42
HCl		-0.671	0.9981	-56.4

Adsorption isotherms variables of inhibitors on XC70 surface in 1M HCl at 25°C, fitted by Voltamaster4 and plotted using OrigiPro 8.

Compounds	Isotherms	Linear equation		R^2	Slope
Fc-1	Langmuir	R_{ct}	$\frac{C}{\theta}$=3.76104E-5+0.97976C	0.96148	0.97976
		C_{dl}	$\frac{C}{\theta}$=0.00154-5.95333C	0.1047	-5.95333
	Temkin	R_{ct}	$\log\left(\frac{C}{\theta}\right)$=4.91184-1.44228θ	0.42461	-1.44228
		C_{dl}	$\log\left(\frac{C}{\theta}\right)$=2.83033+1.50993θ	0.33228	1.50993
	Frumkin	R_{ct}	$\log\left(\frac{\theta}{(1-\theta)C}\right)$=4.08735+0.53443θ	-0.02981	0.53443
		C_{dl}	$\log\left(\frac{\theta}{(1-\theta)C}\right)$=2.81916+2.08471θ	0.53325	2.08471
Fc-2	Langmuir	R_{ct}	$\frac{C}{\theta}$=1.57755E-5+1.14787C	0.9814	1.14787
		C_{dl}	$\frac{C}{\theta}$=1.72324E-4+1.46857C	0.24686	1.46857
	Temkin	R_{ct}	$\log\left(\frac{C}{\theta}\right)$=5.65427-2.35603θ	0.19334	-2.35603
		C_{dl}	$\log\left(\frac{C}{\theta}\right)$=3.38113+0.29328θ	-0.14333	0.29328
	Frumkin	R_{ct}	$\log\left(\frac{\theta}{(1-\theta)C}\right)$=4.83275-0.43879θ	-0.1837	-0.43879
		C_{dl}	$\log\left(\frac{\theta}{(1-\theta)C}\right)$=3.35544+0.92563θ	0.03289	0.92563
Fc-3	Langmuir	R_{ct}	$\frac{C}{\theta}$=4.05804E-5+0.9488C	0.97819	0.9488
		C_{dl}	$\frac{C}{\theta}$=8.47926E-5+1.38949C	0.8473	1.38949
	Temkin	R_{ct}	$\log\left(\frac{C}{\theta}\right)$=4.5674-1.00803θ	0.72111	-1.00803
		C_{dl}	$\log\left(\frac{C}{\theta}\right)$=4.10321-1.07456θ	0.39845	-1.07456
	Frumkin	R_{ct}	$\log\left(\frac{\theta}{(1-\theta)C}\right)$=4.06759+0.56974θ	0.2865	0.56974
		C_{dl}	$\log\left(\frac{\theta}{(1-\theta)C}\right)$=3.97643-0.19041θ	-0.13811	-0.19041

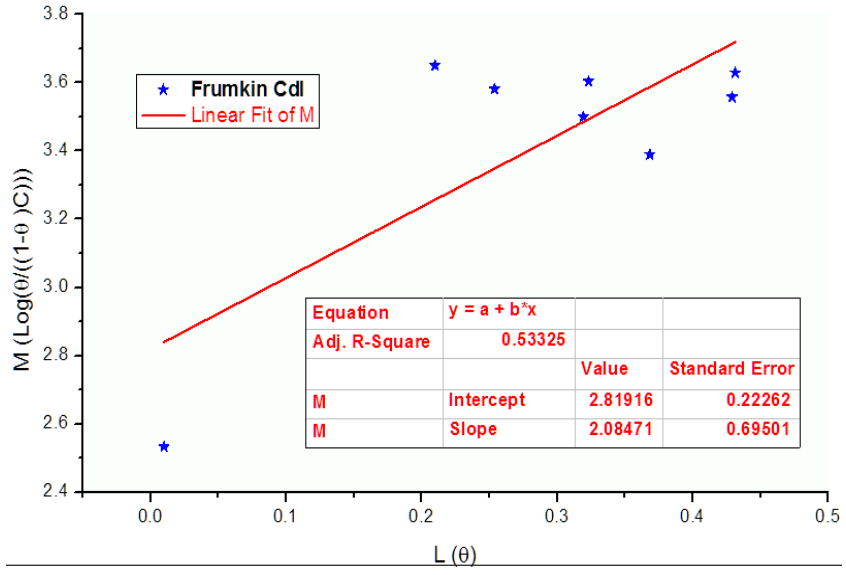

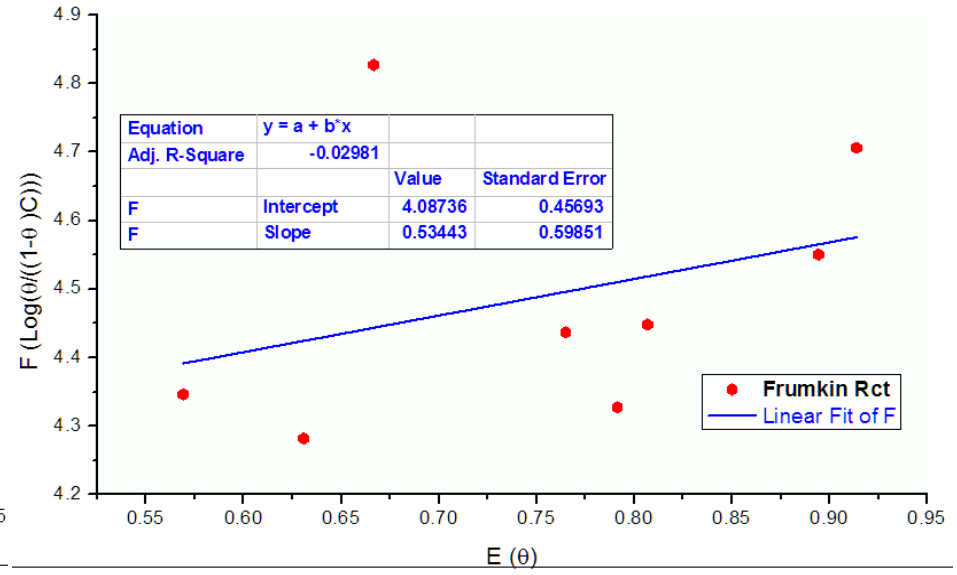

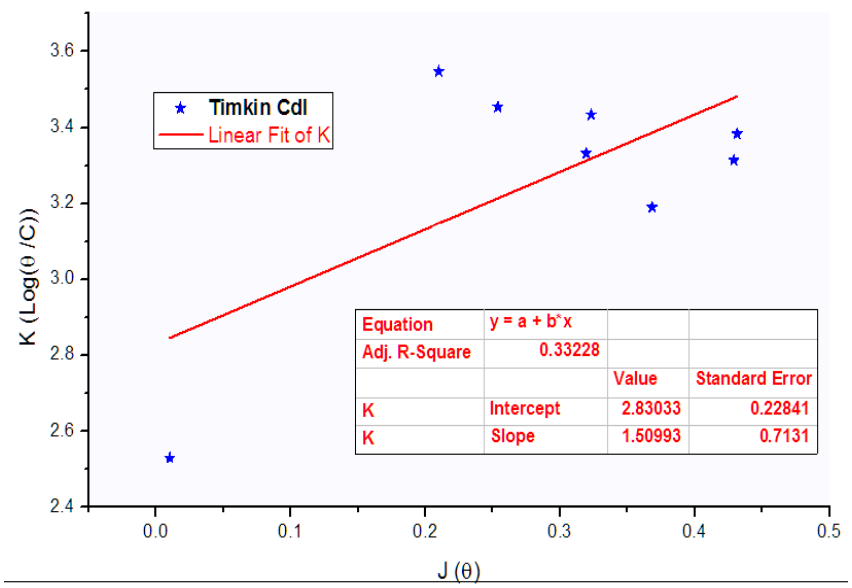

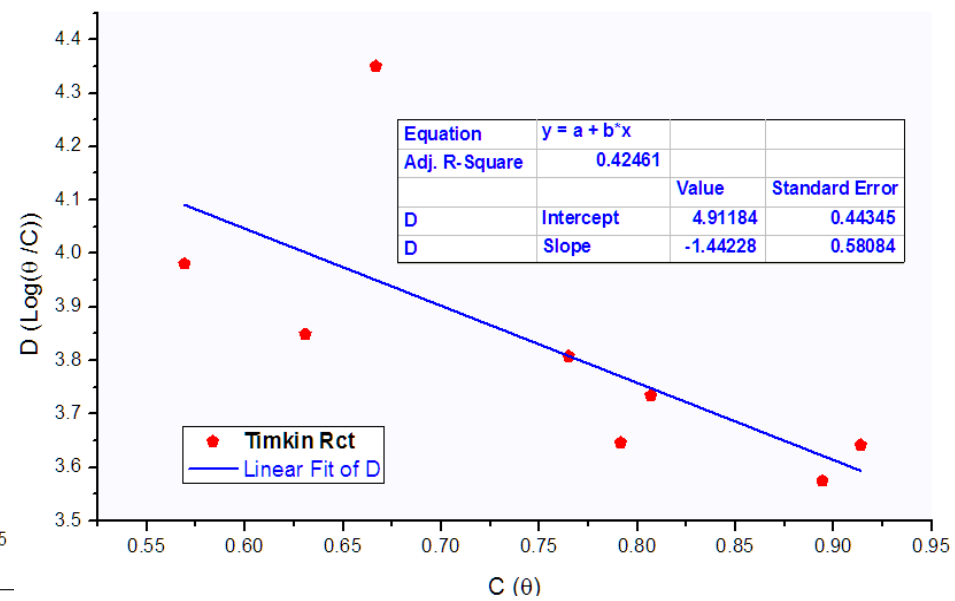

Adsorption isotherms of Fc-1 on XC70 surface in 1M HCl at 25°C fitted by Voltamaster4 and plotted using OrigiPro 8.

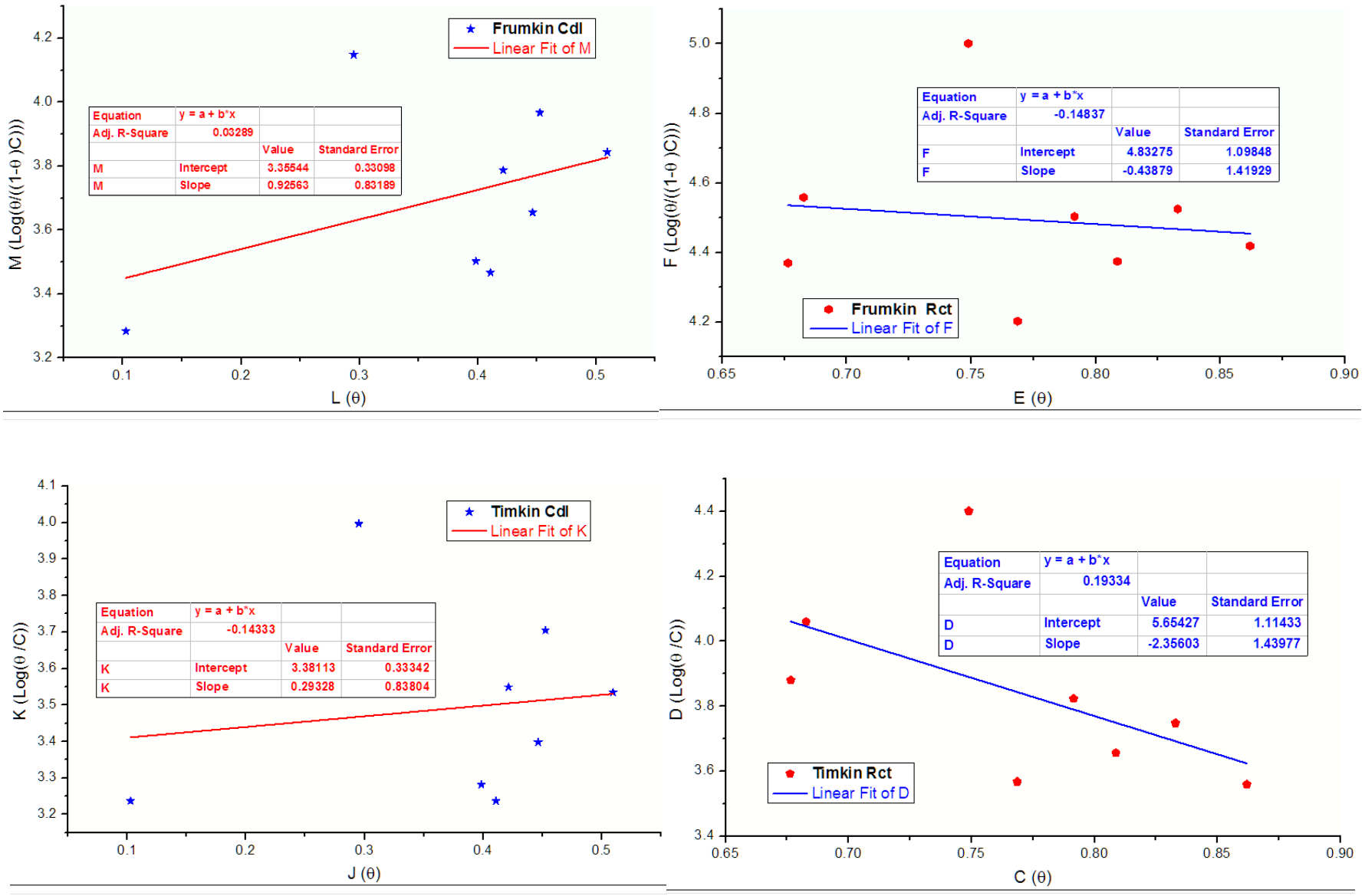

Adsorption isotherms of Fc-2 on XC70 surface in 1M HCl at 25°C fitted by Voltamaster4 and plotted using OrigiPro 8.

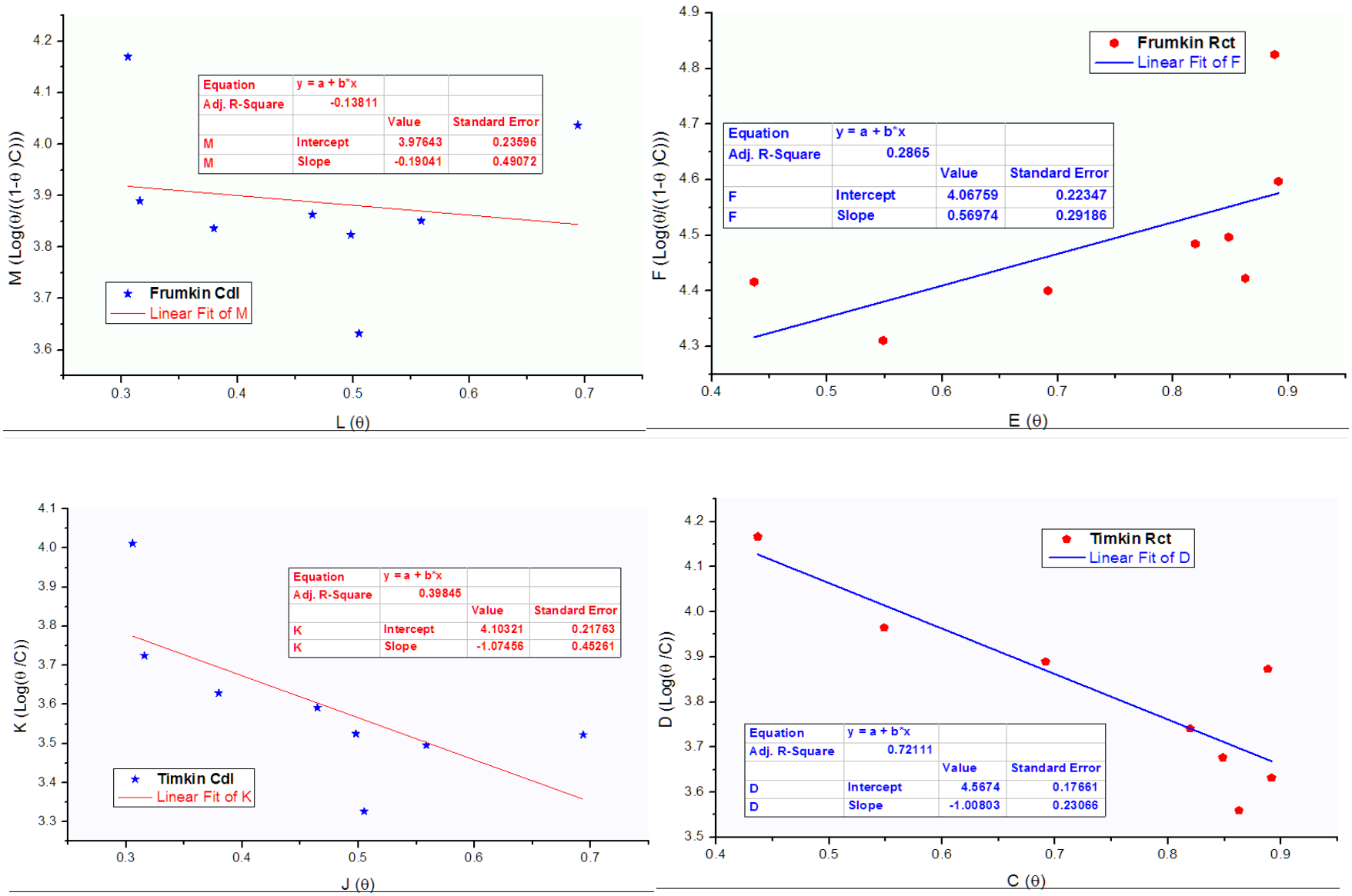

Adsorption isotherms of Fc-3 on XC70 surface in 1M HCl at 25°C fitted by Voltamaster4 and plotted using OrigiPro 8.